SIAM J. MATH. DATA SCI.
Vol. 6, No. 2, pp. 254–282

The Sample Complexity of Sparse Multireference Alignment and Single-Particle Cryo-Electron Microscopy*

Tamir Bendory† and Dan Edidin‡

Abstract. Multireference alignment (MRA) is the problem of recovering a signal from its multiple noisy copies, each acted upon by a random group element. MRA is mainly motivated by single-particle cryo–electron microscopy (cryo-EM) that has recently joined X-ray crystallography as one of the two leading technologies to reconstruct biological molecular structures. Previous papers have shown that, in the high-noise regime, the sample complexity of MRA and cryo-EM is $n = \omega(\sigma^{2d})$, where n is the number of observations, σ^2 is the variance of the noise, and d is the lowest-order moment of the observations that uniquely determines the signal. In particular, it was shown that, in many cases, $d = 3$ for generic signals, and thus, the sample complexity is $n = \omega(\sigma^6)$. In this paper, we analyze the second moment of the MRA and cryo-EM models. First, we show that, in both models, the second moment determines the signal up to a set of unitary matrices whose dimension is governed by the decomposition of the space of signals into irreducible representations of the group. Second, we derive sparsity conditions under which a signal can be recovered from the second moment, implying sample complexity of $n = \omega(\sigma^4)$. Notably, we show that the sample complexity of cryo-EM is $n = \omega(\sigma^4)$ if at most one-third of the coefficients representing the molecular structure are nonzero; this bound is near-optimal. The analysis is based on tools from representation theory and algebraic geometry. We also derive bounds on recovering a sparse signal from its power spectrum, which is the main computational problem of X-ray crystallography.

Key words. sparsity, cryo-EM, multireference alignment, signal processing, representation theory, X-ray crystallography

MSC codes. 94A12, 20C35, 68U10

DOI. 10.1137/23M155685X

1. Introduction.

This paper studies the multireference alignment (MRA) model of estimating a signal from its multiple noisy copies, each acted upon by a random group element. Let V be an orthogonal or unitary representation of a compact group G. Each MRA observation $y \in V$ is drawn from

$$y = g \cdot f + \varepsilon, \tag{1.1}$$

where $g \in G$, $\varepsilon \sim \mathcal{N}(0, \sigma^2 I)$ is a Gaussian noise vector independent of g; $\cdot$ denotes the group action; and $f \in V$. We assume that the distribution of the random element $g \in G$ is uniform (Haar). The goal is to estimate the signal $f \in V$ from n realizations

*Received by the editors March 6, 2023; accepted for publication (in revised form) December 18, 2023; published electronically April 4, 2024.
https://doi.org/10.1137/23M155685X
Funding: This research is supported by the BSF grant 2020159. The first author is also supported in part by the NSF-BSF grant 2019752 and the ISF grant 1924/21, and the second author was also supported by NSF-DMS grant 1906725 and NSF-DMS grant 2205626.

†The School of Electrical Engineering, Tel Aviv University, Tel Aviv 6997801 Israel (bendory@tauex.tau.ac.il).
‡Mathematics, University of Misssouri, Columbia, MO 65211 USA (edidind@missouri.edu).

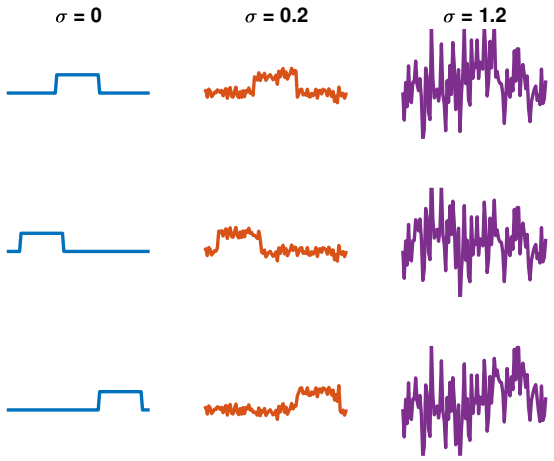

Figure 1. *An example of the one-dimensional MRA setup, where a signal in $\mathbb{R}^N$ is acted upon by random elements of the group of circular shifts $\mathbb{Z}_N$. The left column shows three shifted copies of the signal, corresponding to noiseless measurements (i.e., $\sigma = 0$). In this case, all three observations are admissible solutions because the signal can be estimated only up to a group action. The middle and right columns present the same observations, with low noise level of $\sigma = 0.2$ and high noise level of $\sigma = 1.2$. This paper focuses on the extremely high noise level $\sigma \to \infty$ when the signal is swamped by noise. Figure credit:* [13].

$$y_i = g_i \cdot f + \varepsilon_i \quad i = 1, \dots, n. \tag{1.2}$$

Evidently, given a set of observations $y_1, \dots, y_n$ and with no prior knowledge on f, it is impossible to distinguish between f and $\tilde{g} \cdot f$ for any $\tilde{g} \in G$. Thus, we can only hope to recover the orbit of $f \in V$ under G.

A wide range of MRA models have been studied in recent years. The simplest and most studied model is when a signal in $V = \mathbb{R}^N$ is estimated from its multiple circularly shifted, noisy copies, namely, $G = \mathbb{Z}_N$ [8, 17, 2, 10, 70]. Figure 1 illustrates observations drawn from this model. Additional MRA models include the dihedral group acting on $\mathbb{R}^N$ [20], the group of two-dimensional rotations SO(2) acting on bandlimited images [9, 63, 51], the group of three-dimensional rotations SO(3) acting on bandlimited signals on the sphere [7, 62], and additional setups [71, 49, 21]. The results of this paper hold for any MRA model when a compact group G is acting on a finite-dimensional space V; specific examples are provided in section 2.4.

The MRA model is mainly motivated by single-particle cryo-electron microscopy (cryo-EM), an increasingly popular technology that has joined X-ray crystallography as one of the two leading technologies to reconstruct molecular structures [45, 68]. Under some simplified assumptions, the cryo-EM generative model reads

$$y = T(g \cdot f) + \varepsilon, \quad g \in G, \tag{1.3}$$

where G is the group of three-dimensional rotations SO(3) and T is a tomographic projection acting by

$$Tf(x_1, x_2) = \int_{\mathbb{R}} f(x_1, x_2, x_3) dx_3. \tag{1.4}$$

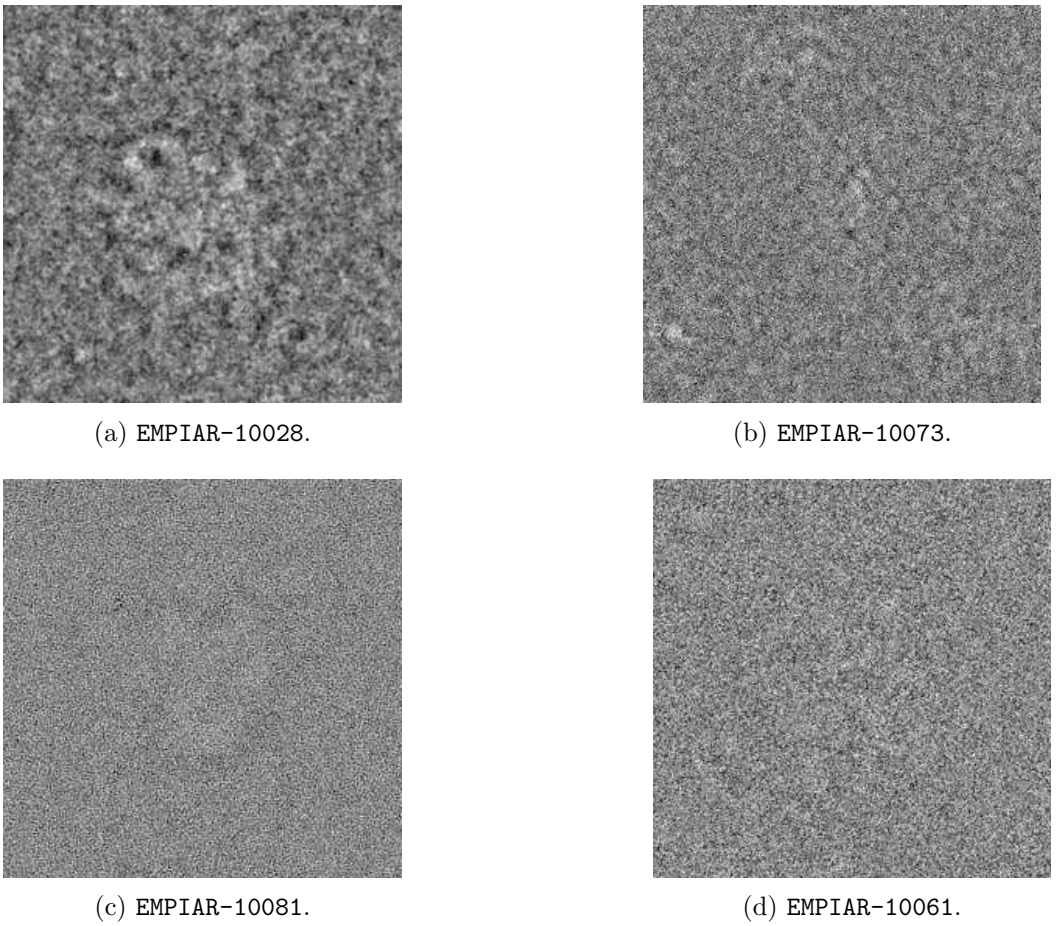

(a) EMPIAR-10028. (b) EMPIAR-10073.

(c) EMPIAR-10081. (d) EMPIAR-10061.

Figure 2. *A collection of cryo-EM experimental images, taken from the Electron Microscopy Public Image Archive (EMPIAR) https://www.ebi.ac.uk/empiar/. The corresponding molecular structures are available at the Electron Microscopy Data Bank (EMDB) https://www.ebi.ac.uk/emdb.* (a) *EMPIAR-10028 (corresponding entry EMD-2660):* Plasmodium falciparum 80*S ribosome bound to the anti-protozoan drug emetine* [91]*;* (b) *EMPIAR-10073 (corresponding entry EMD-8012): yeast spliceosomal U4/U6.U5 tri-snRNP* [67]*;* (c) *EMPIAR-10081 (corresponding entry EMD-8511): human HCN1 hyperpolarization-activated cyclic nucleotide-gated ion channel* [59]*;* (d) *EMPIAR-10061 (corresponding entry EMD-2984): beta-galactosidase in complex with a cell-permeant inhibitor* [11].

The celebrated Fourier slice theorem states that the 2-D Fourier transform of a tomographic projection is equal to a 2-D slice of the volume's 3-D Fourier transform [66]. This motivates analyzing the cryo-EM model in Fourier space, which is indeed the common practice. Notably, the noise level in cryo-EM images is very high; Figure 2 shows several experimental cryo-EM images. We refer the reader to recent surveys on the mathematical and algorithmic aspects of cryo-EM [82, 13, 85].

While the random linear action of 3-D rotation followed by a tomographic projection does not constitute a group action, we will show that the results of this paper apply to the cryo-EM model as well. The emerging molecular reconstruction technology of X-ray free-electron lasers

(XFELs) also obeys (1.3) with one important distinction: The phases in Fourier space are unavailable [87, 64].

MRA analysis in the high- and low-noise regimes. In the low-noise regime, when the signal dominates the noise, the group elements $g_1, \dots, g_n \in G$ can be usually estimated accurately from the observations; see, for example, [81, 27, 32, 74, 61]. If we denote the estimated group elements by $\widehat{g}_1, \dots, \widehat{g}_n \in G$, then an estimator $\widehat{f}$ can be constructed by applying the inverse group elements and averaging

$$\widehat{f} = \frac{1}{n} \sum_{i=1}^{n} \widehat{g}_i^{-1} y_i.$$

In cryo-EM, while the statistical model is more involved (1.3), the group elements can be estimated as well based on the common-lines geometrical property [84, 79], and thus, recovering the molecular structure reduces to a linear inverse problem, for which many effective techniques exist [66].

Motivated by cryo-EM, this work focuses on the high-noise regime when the signal is swamped by noise, and thus, the group elements cannot be accurately estimated [16, 4, 73]. Consequently, one needs to develop methods to estimate the signal f directly, without estimating the group elements as an intermediate step. In particular, two main estimation methods dominate the MRA literature. The first is based on optimizing the marginalized likelihood function, using methods such as expectation maximization [17, 63, 22, 20, 51, 57, 24]. While these techniques are highly successful and are the state-of-the-art methods in cryo-EM [80, 76, 72], their properties are currently not well understood [44, 55, 29, 43]. The second approach is based on the method of moments, a classical parameter estimation technique tracing back to the seminal paper of Pearson [69]. In the method of moments, the idea is to find a signal that is consistent with the empirical moments (which are estimates of the population moments). The method of moments was applied to a wide range of MRA models [17, 7, 70, 2, 31, 28, 63, 71, 5, 49, 62, 22, 20, 24, 46, 1], as well as to construct ab initio models in cryo-EM [25, 26, 60, 77, 16, 58, 50] and XFELs [75, 34]. In this work, we focus on the method of moments due to its appealing statistical properties that are introduced next.

Sample complexity. In the high-noise regime $\sigma \to \infty$, when the dimension of the signal is finite, it was shown that a necessary condition for recovery is $n = \omega(\sigma^{2d})$ (namely, $n/\sigma^{2d} \to \infty$ as $n, \sigma \to \infty$), where d is the lowest-order moment that determines the orbit of the signal uniquely[1] [10, 3, 70]. Therefore, determining the sample complexity in the high-noise regime reduces to analyzing moment equations. In [7, 38], it was shown that, in many cases, if the distribution of the group elements is uniform (as we assume in this paper), $d = 3$ suffices to determine almost all signals, implying sample complexity of $n = \omega(\sigma^6)$; this is also true for cryo-EM. Moreover, in some cases, an efficient algorithm to recover the signal at the optimal estimation rate was devised. For example, if $V \in \mathbb{R}^N$ and $G = \mathbb{Z}_N$, a generic signal can be recovered efficiently from the third moment, called the bispectrum, using a variety of efficient algorithms [17, 70]; see also [62].

[1] This is not necessarily true when the dimension of the signal grows with the noise level and the number of observations [73, 36].

We mention that, when the distribution of the group elements is nonuniform, the MRA problem is usually easier, and signal recovery may be possible from the second moment [2, 20, 77]. In fact, uniform distribution can be thought of as the worst-case scenario of the MRA model (1.1) since, no matter what the original distribution over the group elements is, one can force a uniform distribution by generating a new set of observations:

$$z_i = \tilde{g}_i \cdot y_i = (\tilde{g}_i g_i) \cdot f + \tilde{g}_i \cdot \varepsilon_i, \tag{1.5}$$

where $\tilde{g}_i$ is drawn from a uniform distribution (and thus, the distribution of $\tilde{g}g$ is also uniform). This is not necessarily true for the cryo-EM model.

Main contributions: Signal recovery from the second moment. This work studies signal recovery from the second moment of the MRA observations:

$$\mathbb{E}yy^* = \int_G (g \cdot f)(g \cdot f)^* dg + \sigma^2 I. \tag{1.6}$$

Since we assume that we know σ^2, we henceforth omit the effect of the noise. If we view $g \cdot f$ as a column vector, then $(g \cdot f)(g \cdot f)^*$ is a rank-one matrix, and thus, the second moment is an integral over rank-one Hermitian matrices. Recall that the second moment can be estimated from samples

$$\mathbb{E}yy^* \approx \frac{1}{n} \sum_{i=1}^{n} y_i y_i^*. \tag{1.7}$$

When $n = \omega(\sigma^4)$, $\frac{1}{n}\sum_{i=1}^{n} y_i y_i^*$ almost surely converges to $\mathbb{E}yy^*$. In this paper, we identify a class of signals that are determined uniquely by $\mathbb{E}yy^*$. This, in turn, implies that the sample complexity of the problem, for this class of signals, is $n = \omega(\sigma^4)$, and not $n = \omega(\sigma^6)$ as for generic signals [7, 17, 70].

The first contribution of this paper, introduced in section 2, is a precise characterization of the set of signals having the same second moment. Through the lens of representation theory, we show in Theorem 2.3 that the second moment determines the signal up to a set of unitary matrices whose dimension is governed by the decomposition of the space of signals into irreducible representations of the group. While the unitary matrix ambiguities have been identified before in some special cases [54, 25], we show that the same pattern of ambiguities governs all MRA models. Section 2.4 provides specific examples.

To resolve these ambiguities, we suggest assuming that the signal is sparse under some basis. This is a common assumption in many problems in signal processing and machine learning, such as regression [88, 47], compressed sensing [35, 30, 41], and various image processing applications [40]. Note that the representations of compact groups that we consider are typically spaces of L^2 functions on a domain such as $\mathbb{R}^3$. As such, they do not come equipped with a canonical basis, so the assumption we make is that our signal is sparse with respect to a generic basis. The notion of a generic basis comes from algebraic geometry and makes use of the fact that the set of all possible bases of a vector space is an algebraic variety. When we say that a result holds for a generic basis, it means that there is a Zariski open set of bases for which the statement of the result holds. In particular, it holds for almost all bases. For more detail, see section 3.1.

Our second contribution, presented in section 3 and summarized in Theorem 3.1, describes the sparsity level under which the orbit of a generic sparse signal can be recovered from the second moment; that is, the sparsity level that allows resolving the unknown unitary matrices. This implies that merely $n = \omega(\sigma^4)$ observations are required for accurate signal recovery. The sparsity level is bounded by a factor that depends on the dimensions of the irreducible representations and their multiplicities. The proof of Theorem 3.1 relies on tools from algebraic geometry and representation theory. Specific results are provided in section 3.3.

Implications for cryo-EM. In section 4, we show that the second moment of the cryo-EM model (1.3) is the same as that of the MRA model (1.1) when G is the group of three-dimensional rotations $\mathrm{SO}(3)$ and V is the space of bandlimited functions on the ball. Namely, the tomographic projection operator (1.4) does not change the second moment of the observations. We introduce this model in detail in section 4 and particularize the main result of this paper to cryo-EM in Theorem 4.3. We now state this result informally.

Theorem 1.1 (informal theorem for cryo-EM). *In the cryo-EM model* (1.3) *(described in detail in section* 4.1*), a generic K-sparse function $f \in V$ is uniquely determined by the second moment for $K \lessapprox N/3$, where $N = \dim V$.*

Theorem 1.1 implies that sparse structures can be recovered in the high-noise regime with only $n = \omega(\sigma^4)$ observations, improving upon $n = \omega(\sigma^6)$ for generic structures [7]. Figure 3 shows the distribution of wavelet coefficients (a standard choice of basis in many signal processing applications [65]) of a few molecular structures. Evidently, less than one-third of the coefficients capture almost all the energy of the volumes, suggesting that the bound of Theorem 1.1 is reasonable for typical molecular structures.

A recent paper [23] showed that a structure composed of ideal point masses (possibly convolved with a kernel with a nonvanishing Fourier transform) can be recovered from the second moment. However, the technique of [23] is tailored for this specific model. The same paper also suggests recovering a 3-D structure from the second moment based on a sparse expansion in a wavelet basis. While our results hold for generic bases, and thus not necessarily for any wavelet basis, they provide theoretical support for the numerical results of [23]. Moreover, for a given basis, there is, in principle, a computational technique to test whether Theorem 1.1 holds for that basis. See Remarks 3.2 and 3.3 for more detail.

Crystallographic phase retrieval. The second moment of the MRA model, where random elements of the group of circular shifts $\mathbb{Z}_N$ act on real signals in $\mathbb{R}^N$, is equivalent to the squared absolute values of the Fourier transform of the signal, known as the power spectrum. Recovering a signal from its power spectrum is called the phase retrieval problem, and it has numerous applications in signal processing; see recent surveys and references therein [78, 14, 48, 19].

Crystals are often modeled as functions on a finite abelian group (typically $\mathbb{Z}_N$), which corresponds to the regular representation of the group. For this representation, there is a natural notion of sparsity, which corresponds to requiring that the function is nonzero only on a small subset of elements of the group. Real-valued functions on $\mathbb{Z}_N$ are identified with $\mathbb{R}^N$, and this notion of sparsity corresponds to sparsity in the standard basis of $\mathbb{R}^N$. Recovering a sparse signal from the power spectrum is the main computational challenge in X-ray crystallography, a leading method for elucidating the atomic structure of molecules.

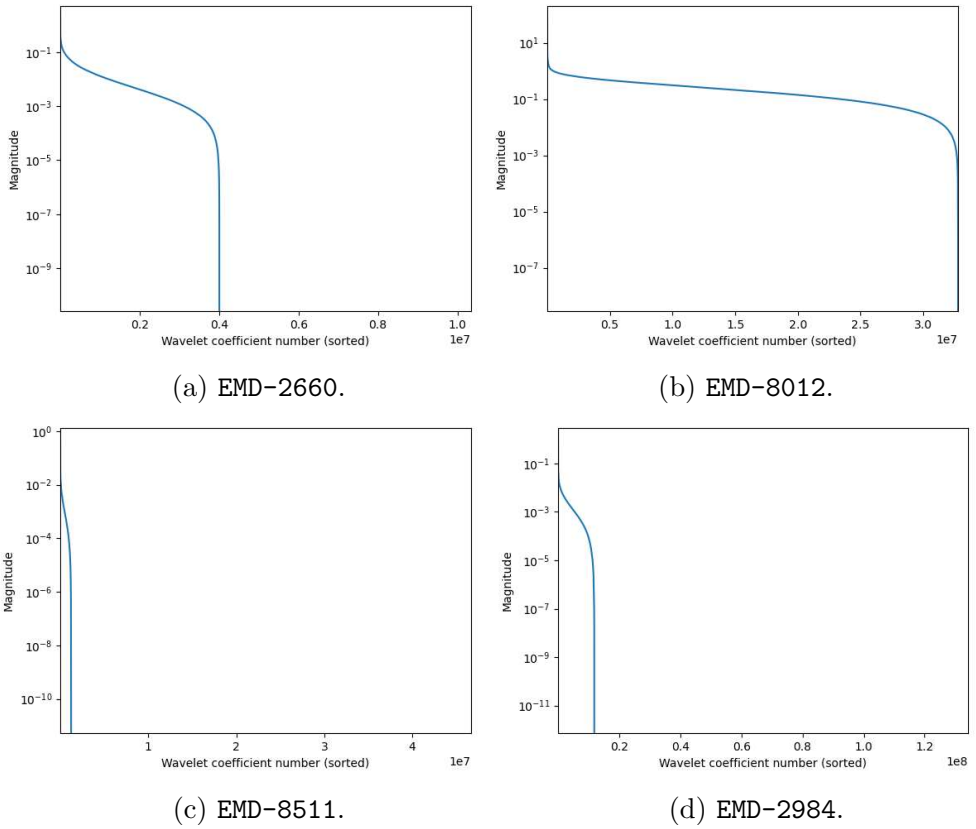

(a) EMD-2660. (b) EMD-8012.

(c) EMD-8511. (d) EMD-2984.

Figure 3. *The sorted wavelet coefficients of cryo-EM structures whose experimental images are presented in Figure 2. The structures were downloaded from the EMDB https://www.ebi.ac.uk/emdb. The structures were expanded using Haar wavelets, where the number of coefficients is approximately the same as the number of voxels. Besides* EMD-8012*, all the volume energy (i.e., the squared norm of the coefficients) is captured by less than one-third of the coefficients, which is the bound of Theorem 1.1. For* EMD-8012*, the same fraction of wavelet coefficients captures more than* 91% *of its energy.*

This is by far the most important phase retrieval application. We discuss this problem in detail in section 5 and explain how the techniques of this paper can be used to prove that a K-sparse signal $f \in \mathbb{R}^N$, under a generic basis, can be recovered from its power spectrum provided that $K \leq N/2$.

Organization of the paper. The rest of the paper is organized as follows. Section 2 formulates the second moment of the MRA model (1.1) and shows that it determines the signal up to a set of unitary matrices. The section also provides several examples. Section 3 derives a bound on the sparsity level that allows for unique recovery from the second moment (Theorem 3.1) in terms of the dimension and multiplicity of the irreducible representations and provides examples. Section 4 focuses on cryo-EM, which is the main motivation of this paper. We formulate the cryo-EM model in detail, derive explicitly the ambiguities of the second moment, and deduce sparsity conditions allowing unique recovery (Theorem 4.3).

Section 5 discusses the crystallographic phase retrieval problem. Section 6 concludes this work and delineates future research directions. The supplementary material (supplement.pdf [local/web 225KB]) provides the necessary background in representation theory.

2. The second moment and symmetries. This section lays out the mathematical background for the second moments of the MRA model (1.1) for a compact group G acting on an N-dimensional real or complex vector space V. Following standard terminology, we refer to a vector space V equipped with an action of a group G as a *representation* of G. Our goal is to use classical methods from the representation theory of compact groups to understand the information obtained from the second moment. In the supplementary material (supplement.pdf [local/web 225KB]), we provide a necessary background in representation theory.

Any representation of a compact group is *unitary*. This means that elements of G act on V as unitary transformations. In particular, the action preserves a Hermitian inner product. By Weyl's unitarian trick, this inner product can be obtained by averaging any chosen inner product on V over the group. If V is a real vector space, then the action of G is *orthogonal*, meaning that elements of G act by orthogonal transformations.

Let $\mathbb{K} = \mathbb{R}$ or $\mathbb{K} = \mathbb{C}$ be the field. Assuming that the distribution on the group G is uniform (Haar), then a choice of basis for an N-dimensional representation $V = \mathbb{K}^N$ expresses the second moment as a function $\mathbb{K}^N \to \mathbb{K}^{N^2}$ given by the formula

$$f \mapsto \int_G (g \cdot f)(g \cdot f)^* dg, \tag{2.1}$$

where $\mathbb{K}^{N^2} = \mathrm{Hom}(V, V)$ is the vector space of linear transformations $V \to V$. The vector f is viewed as a column vector, so $(g \cdot f)(g \cdot f)^*$ is an $N \times N$, rank-one Hermitian matrix.

The second moment can also be defined without the use of coordinates, using tensor notation, as a map $V \to V \otimes V^*$:

$$f \mapsto \int_G (g \cdot f) \otimes \overline{(g \cdot f)} dg. \tag{2.2}$$

We will use both (2.1) and (2.2) interchangeably. The reason that these formulations are equivalent is that there is an isomorphism of representations $V \otimes V^* \to \mathrm{Hom}(V, V)$ as discussed in the supplementary material (supplement.pdf [local/web 225KB]). If we choose an orthonormal basis for V, then the tensor $f_1 \otimes \overline{f_2}$ corresponds to the matrix $f_1 f_2^*$.

Ultimately, we will view elements of V as functions $D \to \mathbb{C}$, where D is some domain on which G acts. For example, in cryo-EM, $G = \mathrm{SO}(3)$, and V is the subspace of $L^2(\mathbb{C}^3)$ consisting of the Fourier transforms of real-valued functions in $L^2(\mathbb{R}^3)$; this problem is discussed in detail in section 4. The second moment of a function $f : D \to \mathbb{C}$ can be viewed as the function $m_f^2 \colon D \times D \to \mathbb{C}$, where

$$m_f^2(x_1, x_2) = \int_G (g \cdot f(x_1))\overline{(g \cdot f(x_2))}\, dg, \tag{2.3}$$

where $g \cdot f \colon D \to \mathbb{C}$ is defined by $gf(x) = f(g^{-1}x)$.

2.1. The second moment of an irreducible representation of G. Recall that a representation is *irreducible* if it has no nonzero proper G-invariant subspaces. Examples of reducible and irreducible representations are given in the supplementary material (supplement.pdf [local/web 225KB]). If the representation V is irreducible, then the following proposition shows that the second moment gives very little information about a vector $f \in V$.

Proposition 2.1. *Let V be an N-dimensional irreducible unitary representation of a compact group G, and identify V with $\mathbb{C}^N$ via a choice of orthonormal basis $f_1, \dots, f_N$ of V. Then, as a map $\mathbb{C}^N \to \mathbb{C}^{N^2}$, the second moment is given by the formula*

$$f \mapsto \frac{|f|^2}{N} I_N, \tag{2.4}$$

where I_N is the $N \times N$ identity matrix. In tensor notation, the second moment is the map $V \mapsto V \otimes V^*$ given by

$$f \mapsto \frac{|f|^2}{N} \sum_{i=1}^{N} f_i \otimes \overline{f_i}. \tag{2.5}$$

Proof. If we identify the Hermitian matrix $m_f^2 = \int_G (g \cdot f)(g \cdot f)^* dg$ as giving a linear transformation $V \to V$, then the second moment defines a map $V \to \mathrm{Hom}(V, V)$, where $\mathrm{Hom}(V, V)$ is the group of linear transformations $V \to V$. Since the second moment is by definition invariant under the action of G on V (i.e., f and $g \cdot f$ both yield the matrix m_f^2), the matrix m_f^2 defines a G-invariant linear transformation on V. However, since V is irreducible, by Schur's lemma, any G-invariant linear transformation $V \to V$ is a scalar multiple of the identity. Since G acts by unitary transformations, $\mathrm{trace}((g \cdot f)(g \cdot f)^*) = \mathrm{trace}(ff^*) = |f|^2$ for any $g \in G$. Thus,

$$\mathrm{trace} m_f^2 = \int_G \mathrm{trace}((g \cdot f)(g \cdot f)^*)\, dg = |f|^2.$$

The formula (2.5) is equivalent to the first formula because, under the identification of $V \otimes V^*$ with $\mathrm{Hom}(V, V) = \mathbb{K}^{N^2}$, the tensor $\sum_{i=1}^{N} f_i \otimes \overline{f_i}$ corresponds to the identity matrix. ∎

2.2. The second moment for multiple copies of an irreducible representation. The following discussion is motivated by the situation in cryo-EM, where we view $\mathbb{R}^3$ as a collection of spherical shells. In other words, we model $\mathrm{SO}(3)$ acting on $L^2(\mathbb{R}^3)$ by taking a number of copies of $L^2(S^2)$. This is a standard model in cryo-EM and is introduced in detail in section 4.

Consider the case where the representation V decomposes as the direct sum of R copies of a single irreducible representation V_0. In other words, there is a G-invariant isomorphism $V \simeq V_0^{\oplus R}$. This means that any vector $f \in V$ can be decomposed uniquely as $f = f[1] + \cdots + f[R]$, with $f[r]$ in the rth copy of V_0. The summands are invariant under the action of G, so $(g \cdot f)[r] = g \cdot f[r]$.

Since V decomposes as the sum $V_0^{\oplus R}$, the tensor product $V \otimes V^*$ decomposes as the sum of tensor products $\oplus_{i,j=1}^{R} V_0[i] \otimes V_0^*[j]$, where $V_0[r]$ indicates the rth copy of V_0 in the decomposition of V. In particular, using tensor notation for the second moment, we can decompose

$$m_f^2 = \int_G (g \cdot f) \otimes \overline{(g \cdot f)} dg = \sum_{i,j=1}^{R} m_f^2[i,j], \tag{2.6}$$

where

$$m_f^2[i,j] = \int_G (g \cdot f[i]) \otimes \overline{(g \cdot f[j])} dg \in V_0[i] \otimes V_0^*[j] \tag{2.7}$$

is the component in the (i,j)th summand of the tensor product $V \otimes V^*$. Each of the summands in (2.7) defines a G-invariant linear transformation $V_0[i] \to V_0[j]$.

Let $N_0 = \dim V_0$. For suitable orthonormal bases $f_1[i], \dots, f_{N_0}[i]$ and $f_1[j], \dots, f_{N_0}[j]$ of $V_0[i]$ and $V_0[j]$, respectively, Schur's lemma implies that

$$m_f^2[i,j] = \int_G (g \cdot f[i]) \otimes \overline{(g \cdot f[j])}\, dg = \frac{\langle f[i], f[j] \rangle}{N} \left(\sum_{k=1}^{N_0} f_k[i] \otimes \overline{f_k[j]} \right).$$

To put this more directly, if we view an element of $V = V_0^{\oplus R}$ as an R-tuple $f[1], \dots, f[R]$ of elements of V_0, then the second moment determines all pairwise inner products $\langle f[i], f[j] \rangle$. Equivalently, if we consider the vectors $f[1], \dots, f[R]$ as the column vectors of an $N_0 \times R$ matrix A, then the second moment determines the $R \times R$ Hermitian matrix A^*A. Therefore, the vectors $f[1], \dots, f[R] \in V_0$ are determined from their pairwise inner products up to the action of the unitary group $U(N_0)$, parameterizing the isometries of V_0. If, as will be the case for cryo-EM, we know that each $f[r]$ lies in a conjugation invariant subspace of V (for example, it is the Fourier transform of a real vector), then we can determine each $f[r]$ up to the action of a subgroup of $U(N_0)$ isomorphic to the real orthogonal group $O(N_0)$.

2.3. The second moment of a general finite-dimensional representation and its group of ambiguities. A general finite-dimensional representation of a compact group can be decomposed as

$$V = \oplus_{\ell=1}^{L} V_\ell^{\oplus R_\ell}, \tag{2.8}$$

where the V_ℓ are distinct (nonisomorphic) irreducible representations of G of dimension N_ℓ. An element of $f \in V$ has a unique G-invariant decomposition as a sum

$$f = \sum_{\ell=1}^{L} \sum_{i=1}^{R_\ell} f_\ell[i], \tag{2.9}$$

where $f_\ell[i]$ is in the ith copy of the irreducible representation V_ℓ. In this case, the second moment decomposes as a sum of tensors $\int_G (g \cdot f_\ell[i]) \otimes \overline{(g \cdot f_m[j])} dg$. Each of these tensors determines a G-invariant map $V_\ell[i] \to V_m[j]$. Since $V_\ell[i]$ and $V_m[j]$ are nonisomorphic irreducible representations, Schur's lemma implies that there are no nonzero G-invariant linear transformations $V_\ell[i] \to V_m[j]$ for $\ell \neq m$. In other words, we have a generalized orthogonality relation that the tensors $\int_G (g \cdot f_\ell[i]) \otimes \overline{(g \cdot f_m[j])}\, dg$ are zero if $\ell \neq m$ for all i, j.

Hence, the second moment decomposes as a sum

$$m_f^2 = \sum_{\ell=1}^{L} \sum_{i,j=1}^{R_\ell} \frac{\langle f_\ell[i], f_\ell[j]\rangle}{N_\ell} \left(\sum_{k=1}^{N_\ell} f_{k,\ell}[i] \otimes \overline{f_{k,\ell}[j]} \right), \tag{2.10}$$

where the vectors $f_{1,\ell}[i], \ldots, f_{N_\ell,\ell}[i]$ form an orthonormal basis for the ith copy of the ℓth irreducible representation V_ℓ.

Remark 2.2. The second moment is a map $V \to \mathrm{Hom}_G(V,V)$. As noted by a referee, $\mathrm{Hom}_G(V,V)$ is the endomorphism ring of the G-module V. A result from classical representation theory, which follows from Schur's lemma, states that this ring decomposes into a sum of matrix algebras $\oplus_{\ell=1}^{L} \mathrm{Mat}(R_\ell)$, and our description of the second moment can also be derived using this decomposition.

2.3.1. Functional representation of the second moment. If, as will be the case for our model of cryo-EM, we view the elements of V as functions $f\colon D \to \mathbb{C}$, then we can reformulate (2.10) as follows. Suppose that $f_{1,\ell}[i], \ldots, f_{N_l,\ell}[i]$ are functions $D \to \mathbb{C}$ that form an orthonormal basis for the ith copy of the ℓth irreducible representation V_ℓ. If we expand $f_\ell[i] = \sum_{m=1}^{N_\ell} A_\ell^m[i] f_{m,\ell}[i]$, then the second moment realized as a function $D \times D \to \mathbb{C}$ is expanded as

$$m_f^2(x_1,x_2) = \sum_{\ell=1}^{L} \sum_{i,j=1}^{R_\ell} \left(\sum_{m=1}^{N_\ell} A_\ell^m[i] \overline{A_\ell^m}[j] \right) \left(\sum_{k=1}^{N_\ell} f_{k,\ell}[i](x_1) f_{k,\ell}^*[j](x_2) \right), \tag{2.11}$$

where x_1, x_2 are, respectively, the variables on the first and second copies of D, respectively.

2.3.2. The group of ambiguities. The main result of this section is a characterization of the group of ambiguities of the second moment. Later on, we provide a few explicit examples.

Suppose that V decomposes as a sum of irreducible representations $V = \oplus_{\ell=1}^{L} V_\ell^{R_\ell}$, where $\dim V_\ell = N_\ell$, and let $H = \prod_{\ell=1}^{L} U(N_\ell)$. The group H acts on V as follows. If $f \in V$ is represented by an L-tuple of $(A_1, \ldots, A_L)$ with A_ℓ an $N_\ell \times R_\ell$ matrix and $h = (U_1, \ldots, U_L)$ with $U_\ell \in U(N_\ell)$, then $h \cdot f = (U_1 A_1, \ldots, U_L A_L)$.

Theorem 2.3. *With the notation as above, a vector $f \in V$ is determined from the second moment up to the action of the ambiguity group $H = \prod_{\ell=1}^{L} U(N_\ell)$. That is, $m_f^2 = m_{f'}^2$ if and only $f = h \cdot f'$ for some $h \in H$.*

Proof. If we decompose a vector $f \in V$ as in (2.9), then the second moment (2.10) determines the inner products $\langle f_\ell[i], f_\ell[j]\rangle$ for all $\ell = 1, \ldots, L$ and $i, j \in 1, \ldots, R_\ell$.

For a general representation, an element of V can be represented by an L-tuple $(A_1, \ldots, A_L)$, where A_ℓ is an $N_\ell \times R_\ell$ complex matrix corresponding to an element in the summand $V_\ell^{\oplus R_\ell}$. The second moment determines the L-tuple of $R_\ell \times R_\ell$ Hermitian matrices $(A_1^* A_1, \ldots, A_L^* A_L)$. Thus, if $U_1, \ldots, U_L$ are unitary matrices, then an L-tuple of $N_\ell \times R_\ell$-matrices $(U_1 A_1, \ldots, U_L A_L)$ has the same second moment because $(U_\ell A_\ell)^*(U_\ell A_\ell) = A_\ell^* A_\ell$ for each ℓ. In particular, a vector f is determined from the second moment up to the action of the product of unitary groups $\prod_{\ell=1}^{L} U(N_\ell)$. ∎

Remark 2.4 (parameter counting). Since each unitary matrix is determined by N_ℓ^2 real parameters, the ambiguity group is of dimension $N_H = \sum_{\ell=1}^{L} N_\ell^2$. If the ambiguity group is isomorphic to the real orthogonal groups, as in cryo-EM, then the ambiguity group is of dimension $N_H = \sum_{\ell=1}^{L} N_\ell(N_\ell - 1)/2$.

Remark 2.5. Note that the total dimension of the ambiguity group of the second moment does not depend on the multiplicities R_ℓ. In particular, the ratio of the dimensions is

$$\frac{N_H}{N} = \frac{\sum_{\ell=1}^{L} N_\ell^2}{2\sum_{\ell=1}^{L} R_\ell N_\ell}.$$

This implies that, as the number of multiplicities increases, the proportional amount of information about the signal contained in the second moment increases as well.

2.4. Examples.

2.4.1. The power spectrum. Consider the group $G = \mathbb{Z}_N$ acting on $\mathbb{K}^N$ by cyclic shifts, where $\mathbb{K} = \mathbb{R}$ or $\mathbb{K} = \mathbb{C}$. In the Fourier domain, the cyclic group $G = \mathbb{Z}_N$ acts by multiplication by roots of unity. In particular, we identify $\mathbb{Z}_N = \mu_N$, where μ_N is the Nth root of unity. If $\omega \in \mu_N$, then

$$\omega \cdot (f[0], \dots, f[N-1]) = (f[0], \omega f[1], \dots, \omega^{N-1} f[N-1]). \tag{2.12}$$

The vector space $\mathbb{C}^N$ with this action of μ_N decomposes as a sum of one-dimensional irreducible representations (namely, $N_\ell = R_\ell = 1$ for all k so that $N = L$) $V_0 \oplus \cdots \oplus V_{N-1}$, where $\omega \in \mu_N$ acts on V_i by $\omega \cdot f[i] = \omega^i f[i]$. The second moment of a vector $f \in \mathbb{C}^N$ in the Fourier domain is the power spectrum $(f[0]|^2, \dots, |f[N-1]|^2)$. This determines the vector up to the action of the group $(S^1)^N$ since $U(1) = S^1$. Figure 4 shows an example of two different images with the same power spectrum.

Recall that the image of $\mathbb{R}^N$ under the discrete Fourier transform is the real subspace of $\mathbb{C}^N$ given by the condition $f[N-i] = \overline{f[i]}$. Thus, if f is the Fourier transform of a real vector,

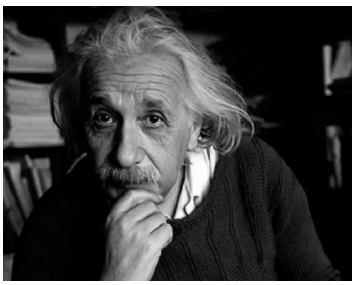

(a) `Einstein`.

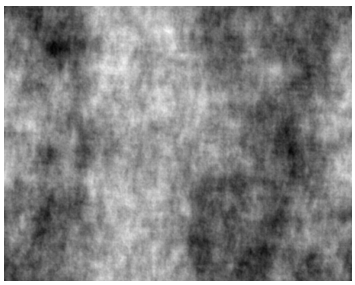

(b) `Einstein with random phases`.

Figure 4. *The left panel shows an image of Albert Einstein. To generate the image of the right panel, we combined the absolute values of the Fourier transform of Einstein's image with random phases and computed the inverse Fourier transform. This example underscores that two images with the same power spectrum may be very different. More generally, two signals that are equal up to a set of unitary matrices (e.g., have the same second moment) may differ significantly.*

the ambiguity group must preserve the condition that $f[N-i] = \overline{f[i]}$ and is therefore the subgroup of

$$\{(\lambda_0, \dots, \lambda_{N-1} | \lambda_{N-n} = \lambda_n^{-1}\} \subset (S^1)^N. \tag{2.13}$$

Recovering a signal from its power spectrum is called the phase retrieval problem [78, 14, 48, 19]; see section 5 for further discussion.

2.4.2. Dihedral MRA. Consider the action of the dihedral group $G = D_{2N}$ acting $\mathbb{K}^N$, where the rotation $r \in D_{2N}$ acts by cyclic shift and the reflection $s \in D_{2N}$ acts by $(s \cdot f)[i] = f[N-i]$. In the Fourier domain, $(s \cdot f)[i] = f[N-i]$ and $(r \cdot f)[i] = \omega^i f[i]$ as in (2.12). In [20], it was shown that the orbit of a generic signal is determined uniquely from the second moment if the group elements are drawn from a nonuniform distribution over the dihedral group. Here, we consider a uniform (Haar) distribution of the group elements.

The vector space $\mathbb{C}^N$ with this action of D_{2N} decomposes into a sum of one- and two-dimensional irreducible representations, depending on the parity of N (with multiplicity $R_\ell = 1$). If N is even, then

$$\mathbb{C}^N = V_0 \oplus V_1 \oplus \cdots V_{N/2-1} \oplus V_{N/2},$$

where V_0 is the one-dimensional subspace spanned by the vector $e_0 = (1, 0, \dots, 0)$, $V_{N/2}$ is spanned by the vector $e_{N/2}$ ($N_0 = N_{N/2} = 1$), and, for $1 \le \ell \le N/2 - 1$, V_ℓ is the subspace spanned by $\{e_\ell, e_{N-\ell}\}$ ($N_\ell = 2$). Similarly, if N is odd, then

$$\mathbb{C}^N = V_0 \oplus V_1 \cdots \oplus V_{(N-1)/2},$$

where again, V_0 is spanned by e_0 and, for $\ell \ge 1$, V_ℓ is spanned by $\{e_\ell, e_{N-\ell}\}$.

Therefore, the second moment of a vector f in the Fourier domain determines the $N/2+1$ real numbers

$$(|f[0]|^2, |f[1]|^2 + |f[N-1]|^2, \dots, |f[N/2-1]|^2 + |f[N/2+1]|^2, |f[N/2]|^2)$$

if N is even and the $(N+1)/2$ real numbers

$$(|f[0]|^2, |f[1]|^2 + |f[N-1]|^2, \dots, |f[(N-1)/2]^2 + |f[(N+1)/2]|^2)$$

if N is odd. When $\mathbb{K} = \mathbb{C}$, this is less information than the power spectrum. When N is even, the ambiguity group is $S^1 \times U(2)^{N/2} \times S^1$, and when N is odd, the ambiguity group is $S^1 \times U(2)^{(N-1)/2}$. However, if $\mathbb{K} = \mathbb{R}$, then the second moment gives the power spectrum because, if f is the Fourier transform of a real vector, then we have $|f[i]| = |f[N-i]|$. In this case, the ambiguity group is $\pm 1 \times O(2)^{N/2} \times \pm 1$ if N is even, and if N is odd, then it is $\pm 1 \times O(2)^{(N-1)/2}$. These groups are isomorphic to the subgroups of $(S^1)^N$ considered in (2.13).

2.4.3. MRA with rotated images. In this model, the Fourier transform of an image is represented as a radially discretized bandlimited function on $\mathbb{C}^2$. That is, our function f is expressed as $f = (f[1], \dots, f[R])$, where

$$f[r](\theta) = \sum_{k=-L'}^{L'} a_{k,r} e^{\iota\theta k}, \quad \theta \in [0, 2\pi), \tag{2.14}$$

for some bandlimit $L' = (L-1)/2$ and R radial samples. The action of a rotation S^1 on the image is given by

$$e^{\iota\alpha} \cdot f[r](\theta) = \sum_{k=-L'}^{L'} a_{k,r} e^{\iota(\theta-\alpha)k} = \sum_{k=-L'}^{L'} a_{k,r} e^{-\iota\alpha k} e^{\iota\theta k}.$$

With this action, the parameter space of two-dimensional images is the S^1-representation $V = V_{-L'}^{\oplus R} \oplus \cdots \oplus V_{L'}^{\oplus R}$, where V_k is the one-dimensional representation of S^1, where $e^{\iota\alpha} \in S^1$ acts with weight $-k$. Namely, $N_k = 1$, $R_k = R$ for all k so that $N = LR$. The (r_1, r_2) component of the second moment equals

$$\begin{aligned} m_f^2[r_1, r_2](\theta_1, \theta_2) &= \int_\alpha e^{-\iota\alpha} f[r_1](\theta_1) \overline{e^{-\iota\alpha} f[r_2](\theta_2)} d\alpha \\ &\quad \int_\alpha \sum_{k_1=-L'}^{L'} a_{k_1,r_1} e^{\iota(\theta_1-\alpha)k_1} \sum_{k_2=-L}^{L} \overline{a_{k_2,r_2}} e^{-\iota(\theta_2-\alpha)k_2} d\alpha \\ &= \sum_{k=-L'}^{L'} a_{k,r_1} \overline{a_{k,r_2}} e^{\iota(\theta_1-\theta_2)k} \\ &= \sum_{k=-L'}^{L'} a_{k,r_1} \overline{a_{k,r_2}} e^{\iota\Delta\theta k} \\ &= m_f^2[r_1, r_2](\Delta\theta), \end{aligned} \tag{2.15}$$

where $\Delta\theta := \theta_1 - \theta_2$. Following our previous discussion, a function $f \in V$ is determined by an L-tuple of $1 \times R$ matrices $(A_{-L'}, \dots, A_{L'})$, where $A_k = (a_{k,1}, \dots, a_{k,R})^T$. The second moment computes the L-tuple of rank-one $R \times R$ matrices $(A_{-L'}^* A_{-L'}, \dots, A_{L'}^* A_L')$. Since each irreducible summand in the representation V has dimension one (namely, $N_\ell = 1$ for all ℓ), the ambiguity group of the second moment for the rotated images problem is $(S^1)^L$. If we assume that the function f is the Fourier transform of a real-valued function, then $a_{k,r} = \overline{a_{-k,r}}$, and the ambiguity group is $O(2)^{L'} \times \pm 1$.

2.4.4. Two-dimensional tomography from unknown random projections. The problem of recovering a two-dimensional image from its tomographic projections is a classical problem in computerized tomography (CT) imaging [66]. However, in some cases, the viewing angles are unknown and may be considered random. Due to the Fourier slice theorem, this is equivalent to randomly rotating the image, and then acquiring a single one-dimensional line of its Fourier transform. While generally, an image cannot be recovered from such random projections (in contrast to the three-dimensional counterpart (1.3), where recovery is theoretically

possible based on the common-lines property [84, 79]), it was shown that unique recovery, up to rotation, requires rather mild conditions [12]. Different algorithms were later developed; see, for example, [33, 86, 93].

In this model, we compute the second moment of the Fourier transform of the image after tomographic projection to a line. In other words, we compute the integral

$$\int_{S^1} Te^{\iota\alpha} \cdot f[r_1](\theta_1) T\overline{e^{\iota\alpha} \cdot f[r_2](\theta_2)} d\alpha,$$

where T is the tomographic projection to the line $\theta = 0$ (the two-dimensional counterpart of (1.4)). Because we are computing the second moment after tomographic projection, we cannot directly determine the ambiguity group from Theorem 2.3. In this case, the tomographic projection causes us to lose information, and we obtain a function only of r_1, r_2 (compare with (2.15)):

$$m_f^2[r_1, r_2] = \sum_{k=-L'}^{L'} a_{k,r_1} \overline{a_{k,r_2}},$$

where $L' = (L-1)/2$. If we view the L-tuple of $1 \times R$ matrices $(A_{-L'}, \dots, A_{L'})$ as a single $L \times R$-matrix A, then the projected second moment determines the Hermitian matrix A^*A. Equivalently, an element of V is determined by R vectors in $\mathbb{C}^L$, and the projected second moment determines all pairwise inner products of these vectors. In this case, the loss of information caused by the tomographic projection means that the ambiguity group is the bigger group $U(L)$ (or $O(L)$ if the image is the Fourier transform of a real-valued function) compared to $(S^1)^L$ in the unprojected case (respectively, $O(2)^{L'} \times \pm 1$).

Remark 2.6. Note that, when $G = \mathrm{SO}(3)$, the second moment is unchanged by the tomographic projection from $\mathbb{R}^3 \to \mathbb{R}^2$. See Lemma 4.1.

3. Retrieving the unitary matrix ambiguities for sparse signals.

In the previous section, we have shown that it is generally impossible to recover a vector f in a representation V of a compact group G from its second moment due to the large group of ambiguities. To resolve these ambiguities and recover the signal in either the MRA (1.1) or cryo-EM (1.3) models, we need a prior on the sought signal. In this work, we assume that the signal is sparse in some basis. This assumption has been studied and harnessed in the MRA [24, 46] and cryo-EM literature [23, 89, 52, 56, 42, 92]. In this section, we derive bounds on the sparsity level that allows retrieving the missing unitary matrices as a function of the dimensions and multiplicities of the irreducible representations. We also provide a couple of examples and leave more detailed discussions on cryo-EM and phase retrieval to, respectively, section 4 and section 5.

3.1. Sparsity conditions.

Let V be an N-dimensional vector space. The notion of sparsity depends on the choice of an orthonormal basis $\mathcal{V} = \{f_1, \dots, f_N\}$. A vector $f \in V$ is K-sparse with respect to this ordered basis if f is a linear combination of at most K elements of this basis. The set of K-sparse vectors with respect to an ordered basis $\mathcal{V}$ is the union of $\binom{N}{K}$ linear subspaces $\mathbb{L}_S(\mathcal{V})$, where $\mathbb{L}_S(\mathcal{V})$ is the subspace spanned by the vectors $\{f_i\}_{i \in S}$ and S is a K-element subset of $[1, N]$.

Let

$$V = \oplus_{\ell=1}^{L} V_\ell^{R_\ell} \tag{3.1}$$

be a representation of a compact group G, where $\dim V_\ell = N_\ell$. Let $H = \prod_{\ell=1}^{L} U(N_\ell)$ be the ambiguity group of the second moment (see Theorem 2.3).

The main result of this section is the following.

Theorem 3.1. *Let V be a representation as in (3.1), let $N = \sum_{\ell=1}^{L} N_\ell R_\ell$ be its total dimension, and let $M = \sum_{\ell=1}^{L} \min(N_\ell R_\ell, N_\ell^2)$. Then, for a generic choice of orthonormal basis $\mathcal{V}$, a generic K-sparse vector $f \in V$ with $K \le N - M$ is uniquely determined by its second moment up to a global phase.*

We note that, as in Remark 2.5, the larger the number of irreducible representation copies is, the easier the problem is. In particular, note that, if $R_\ell \gg N_\ell$ for all ℓ, the sparsity bound reads $K \le \sum_{\ell=1}^{L} R_\ell N_\ell = N$. That is, the sparsity level is proportional to the dimension of the representation. In Theorem 4.3, we provide an explicit example for the cryo-EM case.

Remark 3.2. The set of ordered orthornormal bases of an N-dimensional vector space V can be identified with the real algebraic group $O(N)$ if V is real and $U(N)$ if N is complex. When we say that our result holds for a *generic basis*, we mean that there is a real Zariski open subset of $O(N)$ (resp., $U(N)$) parameterizing bases for which the conclusion of Theorem 3.1 holds. Since the complement of a Zariski open set has Lesbegue measure zero, this means that, given an orthonormal basis $\mathcal{V}$ for V, then, with probability one, Theorem 3.1 holds for that basis.

Remark 3.3. Given a basis $\mathcal{V} = \{f_1, \dots, f_N\}$ for V, we can express $f \in V$ as $\sum_{n=1}^{N} x_i f_i$, and the second moment is a collection of homogeneous quadratic functions in $x_1, \dots, x_N$, which we denote by $m_f^2(x_1, \dots, x_N)$. The following computational test is a simple generalization of the test used in [18, sections 4.3.3 and 4.3.4] that can be used to decide whether $\mathcal{V}$ satisfies the theorem with a sparsity level of K:

If $S \subset [1, N]$ is a subset of size K, let

$$I_S = \{(x_1, \dots, x_N), (y_1, \dots, y_N) | m_f^2(x_1, \dots, x_N) = m_f^2(y_1, \dots, y_N)\} \subset \mathbb{L}_S(\mathcal{V}) \times \mathbb{L}_S(\mathcal{V}),$$

where $\mathbb{L}_S(\mathcal{V})$ is the subspace spanned by $\{f_i\}_{i \in S}$. Likewise, if S, S' are two distinct K-element subsets of $[1, N]$, let

$$I_{S,S'} = \{(x_1, \dots, x_N), (y_1, \dots, y_N) | m_f^2(x_1, \dots, x_N) = m_f^2(y_1, \dots, y_N)\} \subset \mathbb{L}_S(\mathcal{V}) \times \mathbb{L}_{S'}(\mathcal{V}).$$

The conclusion of Theorem 3.1 holds if I_S has dimension exactly K and degree one and $\dim I_{S,S'} < K$. For small values of N, these conditions can be checked using a computer algebra system, but not in polynomial time [18, Appendix D].

Remark 3.4 (frames). Recall that a collection $\mathcal{F}$ of vectors in a finite-dimensional vector space V is a *frame* if the vectors span V. The methods used to prove Theorem 3.1 can also be used to prove a corresponding result where orthonormal bases are replaced by arbitrary frames. The only difference between working with frames instead of bases is that the definition

of a vector being sparse with respect to an ordered frame is more subtle. The reason is that, for a generic frame $\mathcal{F}$, any N-element subset consists of linearly independent vectors, so any $f \in V$ that has zero frame coefficients with respect to N elements in $\mathcal{F}$ must necessarily be zero. In particular, if we work with frames, then the condition that a vector is K-sparse should be replaced by the condition that at least $N-K$ of the frame coefficients are zero. Otherwise, the statements and proofs remain the same.

3.1.1. Strategy and remarks on the proof. The proof of Theorem 3.1 involves a number of steps. Suppose that $\mathcal{V}$ is a generic orthonormal basis, and consider the set of vectors that are K-sparse with respect to $\mathcal{V}$. The set of such vectors forms the union of $\binom{N}{K}$ K-dimensional linear subspaces of V. The strategy of the proof is to show that, with the bounds on K given in the Theorem 3.1, the following is true: If f is a generic K-sparse vector with respect to the orthonormal basis $\mathcal{V}$, the only vectors in the H-orbit of f that are also K-sparse are of the form $e^{\iota\alpha}f$.

Although the H-orbit of f is a real algebraic subvariety of V containing $\{e^{\iota\alpha}f\}$, we know of no general algebraic geometry result that can be used to analyze when a generic linear subspace of V will intersect the orbit Hf exactly in $\{e^{\iota\alpha}f\}$. To prove our result, we will prove something stronger. Rather than consider the H-orbit of a vector f, we will consider the linear span of its orbit and prove that the only K-sparse vectors in the linear span of the orbit of f are scalar multiples of f. The advantage of working with the linear span is that we can use techniques from linear algebra to understand when a linear subspace (the linear span of our orbit) intersects the $\binom{N}{K}$ K-dimensional linear subspaces consisting of vectors that are K-sparse with respect to the given orthonormal basis $\mathcal{V}$.

The price we pay for working with the linear span of an orbit instead of directly working with the orbit is that, if the H orbit of f has real dimension M, then its linear span is a complex linear subspace of complex dimension M or equivalently real dimension $2M$ (see Proposition 3.5). As a result, the sparseness bound we obtain may not be optimal. However, when $\dim H << \dim V$, as is the case in cryo-EM, this gap is not significant.

Finally, we remark that, for the general MRA problem with group G (1.1), we can at best recover the G-orbit of a vector f from its moments. However, by imposing the prior condition that the vector is sparse with respect to a given basis, we have the possibility of recovering a vector up to a global phase. The reason is that, for a general orthonormal basis $\mathcal{V}$ of V, the sparse vectors are not invariant under the action of G.

3.2. Proof of Theorem 3.1. Let H be a group acting on a vector space V and $f \in V$ any vector. We denote by $\mathbb{L}_f$ the *linear span* of the H-orbit Hf. By definition, $\mathbb{L}_f = \{\sum a_i(h_i \cdot f) | a_i \in \mathbb{C}, h_i \in H\}$, and it is the smallest linear subspace containing the orbit Hf.

Let $V = \oplus_{\ell=1}^{L} V_\ell^{R_\ell}$ be a unitary representation of a compact group G, and let $H = \prod_{\ell=1}^{L} U(N_\ell)$. Given a vector $f \in V$, we can write $f = \sum_{\ell=1}^{L}\sum_{r=1}^{R_\ell} f_\ell[r]$, where $f_\ell[r]$ is in the rth copy of the irreducible representation V_ℓ. As above, we can view our vector f as an L-tuple $(A_1, \dots, A_L)$ of $N_\ell \times R_\ell$ matrices with $A_\ell = \big(f_\ell[1])^T, \dots, (f_\ell[R_\ell])^T\big)$. Viewing $V_\ell^{R_\ell}$ as the vector space of $N_\ell \times R_\ell$ matrices, the linear span $\mathbb{L}_f$ of the orbit Hf is the product of the linear spans of the $U(N_\ell)$ orbits of the matrices A_ℓ, where elements of $U(N_\ell)$ act on A_ℓ by left multiplication.

Proposition 3.5. *Let $V = \oplus_\ell^L V_\ell^{R_\ell}$ be a unitary representation of a compact group G, and let $H = \prod_{\ell=1}^L U(N_\ell)$. If $f \in V$ is represented by an L-tuple $(A_1, \dots, A_L)$ of $N_\ell \times R_\ell$ matrices, then*

$$\dim_{\mathbb{C}} \mathbb{L}_f = \sum_{\ell=1}^{L} (\text{rank} A_\ell) N_\ell,$$

where $\dim_{\mathbb{C}}$ denotes the dimension of $\mathbb{L}_f$ as a complex vector space. In particular,

$$\dim_{\mathbb{C}} \mathbb{L}_f \leq \sum_{\ell=1}^{L} M_\ell,$$

where $M_\ell = \min(N_\ell R_\ell, N_\ell^2)$.

Proof. Since the linear span of the H-orbit of $f = (A_1, \dots, A_L)$ is the product of the linear spans of the $U(N_\ell)$-orbits of the matrices A_ℓ, it suffices to prove that the linear span of the $U(N_\ell)$-orbit of the matrix A_ℓ in $V_\ell^{R_\ell}$ has dimension $(\text{rank} A_\ell) N_\ell$.

Let $r_\ell = \text{rank} A_\ell$, and, to simplify notation, assume that the first r_ℓ columns $f_\ell[1]^T, \dots, f_\ell[r_\ell]^T$ of A_ℓ are linearly independent. Since $\text{rank} A_\ell = r_\ell$, for $r > r_\ell$, there are unique scalars $b_{1,r}, \dots, b_{r_\ell,r}$ such that $f_\ell[r] = \sum_{i=1}^{r_\ell} b_{i,r} f_\ell[i]$.

Let $\mathbb{L}_{A_\ell}$ be the $r_\ell N_\ell$-dimensional linear subspace of $V_\ell^{R_L}$ consisting of $N_\ell \times R_\ell$ matrices B such that, for $r > r_\ell$, $B_r = \sum_{i=1}^{r_\ell} b_{i,r} B_i$, where B_i denotes the ith column of the matrix B. Since $U(N_\ell)$ acts linearly, the linear relations on the columns of A_ℓ are preserved by the action of $U(N_\ell)$, so the linear span of $U(N_\ell)A_\ell$ lies in the subspace $\mathbb{L}_{A_\ell}$. Conversely, we note that the linear span of $U(N_\ell)A_\ell$ contains the open set $\mathbb{L}_{A_\ell}^o$ of $\mathbb{L}_{A_\ell}$, parameterizing matrices whose first r_ℓ columns are linearly independent. The reason this holds is that any invertible $N_\ell \times N_\ell$ matrix is a linear combination of unitary matrices, and any element of $\mathbb{L}_{A_\ell}^o$ can be obtained by applying some invertible matrix to A_ℓ. ∎

Remark 3.6. Note that the real dimension of the $U(N_\ell)$-orbit of the matrix A_ℓ considered in the proof of Proposition 3.5 has real dimension $r_\ell N_\ell$. It follows that, for any vector $f \in V$, $\dim_{\mathbb{C}} \mathbb{L}_f = \dim_{\mathbb{R}} Hf$. In particular, the real dimension of $\mathbb{L}_f$ is twice the real dimension of the orbit Hf.

To prove the theorem, we need to show that the set $\mathcal{U}$ of orthonormal bases $\mathcal{V}$ such that, for every subset $S \subset [1, N]$ with $|S| = K$ and with $K \leq M = \sum_{\ell=1}^L \min(N_\ell R_\ell, N_\ell^2)$, the following statements hold.

1. For generic $f \in \mathbb{L}_S(\mathcal{V}), \mathbb{L}_f \cap \mathbb{L}_S(\mathcal{V})$ is the line spanned by f.
2. For generic $f \in \mathbb{L}_S(\mathcal{V})$, if $|S'| = K$ and $S' \neq S$, then $\mathbb{L}_f \cap \mathbb{L}_S(\mathcal{V}) = \{0\}$.

For a fixed subset S with $|S| = K$, let $\mathcal{U}_S$ be the set of orthonormal bases such that (1) and (2) hold for S. Then, $\mathcal{U} = \cap_S \mathcal{U}_S$. Since the intersection of a finite number of Zariski open sets is Zariski open, it suffices to prove that each $\mathcal{U}_S$ contains a Zariski open set. Moreover, the proof is identical up to indexing for each subset S, so we will assume, for simplicity of notation, that $S = \{1, \dots, K\}$.

Given a vector $f \in V$, let $\mathcal{B}_f$ be the set of orthonormal bases such that $f \in \mathbb{L}_{\{1,\dots,K\}}$. Note that $\mathcal{B}_f$ is a Zariski closed subset of $O(N)$ (resp., $U(N)$) defined by the equation $f_1 \wedge \cdots \wedge f_K \wedge f = 0$, where $f_1, \dots, f_K$ are the first K vectors of an ordered basis.

Proposition 3.7. *Let $f \in V$ be any nonzero vector, and let $\mathbb{L}_f$ be the linear span of its orbit under H. Let $M = \sum_{\ell=1}^{L} \min(N_\ell R_\ell, N_\ell^2)$. Then, if $K \leq N - M$, for the generic orthonormal basis $\mathcal{V} \in \mathcal{B}_f$,*

(1) *$\mathbb{L}_f$ intersects $\mathbb{L}_{\{1,\dots,K\}}(\mathcal{V})$ in the line spanned by f;*
(2) *$\mathbb{L}_f \cap \mathbb{L}_S(\mathcal{V}) = \{0\}$ if $S \neq \{1,\dots,K\}$.*

The set of orthonormal bases $\mathcal{V} \in \mathcal{B}_f$ for which conditions (1) and (2) of Proposition 3.7 are not satisfied is defined by polynomial equations. This means that the set of bases satisfying (1) and (2) is Zariski open, and, to prove Proposition 3.7, we just need to show that this set is nonempty; i.e., we just need to show that there exists a basis $\mathcal{V} \in \mathcal{B}_f$ that satisfies conditions (1) and (2). To do this, we need to introduce some notation and prove a lemma.

Fix an orthonormal basis $e_1, \dots, e_N$ of a Hermitian vector space V of dimension N. For $S \subset [1, N]$ with $|S| = K$, let $\mathbb{L}_S = \operatorname{span}\{e_i\}_{i \in S}$ and $\mathbb{L}_S^*$ be the open subset of $\mathbb{L}_S$ of vectors whose expansion with respect to the basis $\{e_i\}_{i \in S}$ has all nonzero coordinates. In other words, $\mathbb{L}_S^* = \mathbb{L}_S \setminus (\bigcup_{S' \neq S} \mathbb{L}_{S'})$.

For a given vector $w \in V$, let $\operatorname{Gr}_w(M, V)$ be the subvariety of the Grassmannian of M-dimensional linear subspaces of V that contain w.

Lemma 3.8. *If $K \leq N - M$, then, for any vector $w \in \mathbb{L}_{\{1,\dots,K\}}^*$, the generic M-dimensional linear subspace $\mathbb{L} \in \operatorname{Gr}_w(M, V)$ satisfies the following conditions:*

1. *$\mathbb{L} \cap \mathbb{L}_{\{1,\dots,K\}}$ is the line spanned by w;*
2. *$\mathbb{L} \cap \mathbb{L}_S = \{0\}$ for $S \neq \{1,\dots,K\}$ and $|S| = K$.*

Proof of Lemma 3.8. The subset of $\operatorname{Gr}_w(M, V)$ parameterizing linear subspaces intersecting $\mathbb{L}_{\{1,\dots,K\}}$ in dimension greater than one is locally defined by a polynomial equation and therefore a proper algebraic subset. Likewise, for any $S \neq \{1,\dots,K\}$, the subset of $\operatorname{Gr}_w(M, V)$ parameterizing linear subspace $\mathbb{L}$ such that $\mathbb{L} \cap \mathbb{L}_S \neq \{0\}$ is also defined by a polynomial equation and thus is again a proper algebraic subset. In particular, the set of $\mathbb{L} \in \operatorname{Gr}_w(M, V)$ that do not satisfy conditions (1) and (2) lie in a proper algebraic subset of $\operatorname{Gr}_w(M, V)$. Therefore, the generic subspace $\mathbb{L} \in \operatorname{Gr}_w(M, V)$ satisfies conditions (1) and (2). ∎

Proof of Proposition 3.7. Choose a fixed orthonormal basis $\{e_1, \dots, e_N\}$, and let $(\mathbb{L}, w)$ be an M-dimensional linear subspace and vector satisfying the conclusions (1) and (2) of Lemma 3.8. If we choose w so that $|w| = |f|$, then we can find a rotation $g \in U(N)$ such that $g \cdot (\mathbb{L}, w) = (\mathbb{L}_f, f)$. The orthonormal basis $\{v_i = g \cdot e_i\}_{i=1,\dots,N}$ satisfies conditions (1) and (2) of the proposition. ∎

Proposition 3.9. *Let $\mathcal{V}$ be an ordered orthonormal basis for V, and assume that there is a nonzero vector $f_0 \in L_{\{1,\dots,K\}}(\mathcal{V})$ such that $\dim \mathbb{L}_{f_0} \cap \mathbb{L}_{\{1,\dots,K\}}(\mathcal{V}) = 1$ and $\mathbb{L}_{f_0} \cap \mathbb{L}_S(\mathcal{V}) = \{0\}$ for $S \neq \{1,\dots,K\}$. Then, for a generic $f \in \mathbb{L}_{\{1,\dots,K\}}(\mathcal{V})$, the same property holds.*

Proof. Given an orthonormal basis $\mathcal{V}$, the set D of $f \in \mathbb{L}_{\{1,\dots,K\}}(\mathcal{V})$, which satisfies the condition that $\dim \mathbb{L}_f \cap \mathbb{L}_{\{1,\dots,K\}}(\mathcal{V}) > 1$ or $\dim \mathbb{L}_f \cap \mathbb{L}_S(\mathcal{V}) > 0$ for $S \neq \{1,\dots,K\}$, is defined by polynomial equations. By hypothesis, we know that $D \neq \mathbb{L}_{\{1,\dots,K\}}$ since $f_0 \notin D$, so its complement is necessarily Zariski dense. ∎

At this point, we have proved the following. For a fixed vector nonzero $f_0 \in V$, there is a Zariski open set $\mathcal{U}_{f_0} \subset \mathcal{B}_{f_0}$ such that, for every $\mathcal{V} \in \mathcal{U}_{f_0}$, the generic vector $f \in \mathbb{L}_{\{1,\dots,K\}}$ satisfies conditions (1) and (2) of Proposition 3.7.

To complete the proof, we observe that the set of all bases is $\bigcup_{f_0 \in \mathbb{P}(V)} \mathcal{B}_{f_0}$, and our desired set of bases is $\bigcup_{f_0 \in \mathbb{P}(V)} \mathcal{U}_{f_0}$, where $\mathbb{P}(V)$ is the projective space of lines in V. This set is open in $O(N)$ (resp., $U(N)$) because it is the image under the projection of the complement of the Zariski closed set $Z = \{(\mathcal{V}, f) | \mathcal{V} \in (\mathcal{B}_f \setminus \mathcal{U}_f)\}$ in the universal frame bundle $\{(\mathcal{V}, f) | f \in \mathcal{V}\} \subset O(N) \times \mathbb{P}(V)$ (resp., $U(N) \times \mathbb{P}(V)$), and this projection is open (meaning that it takes Zariski open sets to Zariski open sets) because it is flat.

3.3. Examples.

3.3.1. MRA with rotated images model. Using Theorem 3.1, we can obtain sparsity bounds for recovering a generic image from its second moment as in section 2.4.3.

Recall that, in this model, the Fourier transform of an image is represented as a radially discretized bandlimited function on $\mathbb{C}^2$, and the function f is determined by an L-tuple $(A_{-L'}, \dots, A'_L)$ vector in $\mathbb{C}^R$, where $L' = (L-1)/2$ is the bandlimit and R is the number of radial samples. The ambiguity group is $H = (S^1)^{2L+1}$. In the notation of Theorem 3.1, we have $M_\ell = 1$ for $\ell = -L', \dots, L'$. In particular, for any vector $f \in V$, $\dim \mathbb{L}_f \leq L$. Hence, by Theorem 3.1 we can conclude that, if $K \leq \dim V - L$, then, for a generic orthonormal basis, a generic K-sparse vector can be recovered from its second moment. Since $\dim V = RL$, if the number of radial samples $R \geq 2$, then the sparsity level required for signal recovery is $K \leq \frac{R-1}{R} N$, namely, linear in $\dim V$. If only one radial sample is taken ($R = 1$), then this problem reduces to the MRA model on the circle, which is equivalent to the Fourier phase retrieval problem [14].

3.3.2. Sparsity bounds for two-dimensional tomography from unknown random projections. Following the model of section 2.4.4, the unknown image f is viewed as an $L \times R$ matrix A, and the projected second moment determines the matrix A^*A. Thus, the ambiguity group is $U(L)$ (complex images) or $O(L)$ (real images). The orbit of a generic signal f has dimension M, where $M = \min(\dim V, L^2)$. Since $\dim V = LR$, we have $M = \min(RL, L^2)$. In order to be able to recover sparse signals, we need to take $R > L$; i.e., the number of radial samples must exceed the number of frequencies. Specifically, Theorem 3.1 implies that, for a generic ordered orthonormal basis $\mathcal{V}$, we can recover K-sparse signals where $K = (R-L)L$. In particular, if $R > pL$ with $p > 1$, then a generic K-sparse signal is uniquely determined by its second moment if $K \leq \frac{p-1}{p} N$, where $N = \dim V$.

4. Application to cryo-EM.

This section is devoted to the application of the results of section 2 and section 3 to single-particle cryo-EM, which is the main motivation of this work.

Recent technological breakthroughs in cryo-EM have sparked a revolution in structural biology—the field that studies the structure and dynamics of biological molecules—by recovering an abundance of new molecular structures at near-atomic resolution. In particular, cryo-EM allows recovering molecules that were notoriously difficult to crystallize (e.g., different types of membrane proteins), the sample preparation procedure is significantly simpler (compared to alternative technologies) and preserves the molecules in a near-physiological state, and it allows reconstruction of multiple functional states.

In this section, we describe the mathematical model of cryo-EM in detail, formulate the ambiguities of recovering the three-dimensional structure from the second moment, and then derive the sparsity level that allows resolving these ambiguities based on Theorem 3.1.

4.1. Mathematical model. Let $L^2(\mathbb{R}^3)$ be a Hilbert space of complex-valued L^2 functions on $\mathbb{R}^3$. The action of SO(3) on $\mathbb{R}^3$ induces a corresponding action on $L^2(\mathbb{R}^3)$, which we view as an infinite-dimensional representation of SO(3). In cryo-EM, we are interested in the action of SO(3) on the subspace of $L^2(\mathbb{R}^3)$ corresponding to the Fourier transforms of real-valued functions on $\mathbb{R}^3$, representing the Coulomb potential of an unknown molecular structure.

Using spherical coordinates (r,θ,ϕ) we consider a finite-dimensional approximation of $L^2(\mathbb{R}^3)$ by discretizing $f(r,\theta,\phi)$ with R samples $r_1,\dots,r_R$ of the radial coordinates and bandlimiting the corresponding spherical functions $f(r_i,\theta,\phi)$. This is a standard assumption in the cryo-EM literature; see, for example, [9]. Mathematically, this means that we approximate the infinite-dimensional representation $L^2(\mathbb{R}^3)$ with the finite-dimensional representation $V=(\oplus_{\ell=0}^{L}V_\ell)^R$, where L is the bandlimit, and V_ℓ is the $(2\ell+1)$-dimensional irreducible representation of SO(3), corresponding to harmonic polynomials of frequency ℓ. An orthonormal basis for V_ℓ is the set of spherical harmonic polynomials $\{Y_\ell^m(\theta,\phi)\}_{m=-\ell}^{\ell}$. We use the notation $Y_\ell^m[r]$ to consider the corresponding spherical harmonic as a basis vector for functions on the rth spherical shell. The dimension of this representation is $R(L^2+2L+1)$.

Viewing an element of V as a radially discretized function on $\mathbb{R}^3$, we can view $f\in V$ as an R-tuple

$$f=(f[1],\dots,f[R]),$$

where $f[r]\in L^2(S^2)$ is an L-bandlimited function. Each $f[r]$ can be expanded in terms of the basis functions $Y_\ell^m(\theta,\varphi)$ as follows:

$$f[r]=\sum_{\ell=0}^{L}\sum_{m=-\ell}^{\ell}A_\ell^m[r]Y_\ell^m. \tag{4.1}$$

Therefore, the problem of determining a structure reduces to determining the unknown coefficients $A_\ell^m[r]$ in (4.1).

Note that, when f is the Fourier transform of a real-valued function, the coefficients $A_\ell^m[r]$ are real for even ℓ and purely imaginary for odd ℓ [25].

4.2. The second moment of the cryo-EM model. In this section, we first formulate the second moment of the MRA model (1.1) for $G=\mathrm{SO}(3)$ and functions of the form (4.1). Then, we show that this is equivalent to the second moment of the cryo-EM model (Lemma 4.1) and derive the ambiguity group of this model (Corollary 4.2).

Consider the MRA model with $G=\mathrm{SO}(3)$ and functions of the form (4.1). Using the expansion from the previous section and the functional representation of the second moment (2.11), we can write

$$m_f^2=\sum_{r_1,r_2=1}^{R}\sum_{\ell=0}^{L}\left(\sum_{m=-\ell}^{\ell}A_\ell^m[r_1]\overline{A_\ell^m[r_2]}\right)\sum_{m'=-\ell}^{\ell}Y_\ell^{m'}[r_1]\overline{Y_\ell^{m'}[r_2]}, \tag{4.2}$$

where the notation $Y_\ell^m[r]$ denotes the corresponding spherical harmonic in the rth copy of $V_\ell\subset L^2(S^2)$. To simplify notation, set

$$B_\ell[r_1,r_2]=\sum_{m=-\ell}^{\ell}A_\ell^m[r_1]\overline{A_\ell^m[r_2]}. \tag{4.3}$$

This can be viewed as an inner product of the coefficient vector $(A_\ell^{-\ell}[r_1],\dots,A_\ell^{\ell}[r_1])$ from the r_1 shell and the coefficient vector $(A_\ell^{-\ell}[r_2],\dots,A_\ell^{\ell}[r_2])$ from the r_2 shell. Let $A_\ell \in \mathbb{C}^{(2\ell+1)\times R}$ and $B_\ell \in \mathbb{C}^{R\times R}$ be matrices consisting of the coefficients

$$A_\ell = (A_\ell^m[r_i])_{m=-\ell,\dots,\ell,i=1,\dots,R}$$

and

$$B_\ell = (B_\ell[r_i,r_j])_{i,j=1,\dots,R}.$$

Then, the second moment determines the matrices

$$B_\ell = A_\ell^T A_\ell, \quad \ell = 0,\dots,L. \tag{4.4}$$

Remarkably, unlike the tomographic projection $\mathbb{R}^2 \to \mathbb{R}^1$, the tomographic projection operator (1.4) does not affect the second moment for SO(3). Therefore, in the context of the second moment, we can treat cryo-EM as a special case of the MRA model (1.1), where G is the group of three-dimensional rotations SO(3) and V is a discretization of $L^2(\mathbb{R}^3)$ as in (4.1). This fact has been recognized (implicitly) already by Zvi Kam [54]. For completeness, we prove the following lemma.

Lemma 4.1. *Assume a function of the form (4.1). Then, the second moment of the cryo-EM model (1.3) is the same as the second moment of the MRA model (1.1) with $G = SO(3)$. Namely, the tomographic projection operator in (1.3) does not affect the second moment.*

Proof. Consider the projected second moment of a function $f \in V$ for fixed (r_1,r_2):

$$\begin{aligned}
&\int_{\mathrm{SO}(3)} T(g\cdot f[r_1](\theta_1,\phi_2))T(\overline{g\cdot f[r_2](\theta_2,\phi_2)})\,dg \\
&\quad = (T\times T)\int_{\mathrm{SO}(3)} (g\cdot f[r_1](\theta_1,\phi_1)\overline{(g\cdot f[r_2])(\theta_2,\phi_2)})dg \\
&\quad = (T\times T)(m_f^2[r_1,r_2](\theta_1,\phi_1,\theta_2,\phi_2)) \\
&\quad = \sum_{\ell=0}^{L} B_\ell[r_1,r_2] \sum_{m=-\ell}^{\ell} Y_\ell^m(\pi/2,\varphi_1)[r_1]\overline{Y_\ell^m(\pi/2,\varphi_2)[r_2]}.
\end{aligned} \tag{4.5}$$

Here, $T\times T$ is the product of tomographic projections so that $(T\times T)f(\theta_1,\phi_1,\theta_2,\phi_2) = f(\pi/2,\phi_1,\pi/2,\phi_2)$. Note that the first equality holds because the linear operator T commutes with integration over the group SO(3). Let P_ℓ be the Legendre polynomial of degree ℓ. Since, up to constants [6, section 2.2],

$$\sum_{m=-\ell}^{\ell} Y_\ell^m(\pi/2,\varphi_1)\overline{Y_\ell^m(\pi/2,\varphi)} = P_\ell(\cos(\varphi_1-\varphi_2)), \tag{4.6}$$

we have

$$\int_G T(g\cdot f[r_1])\overline{T(g\cdot f[r_2])}\,dg = \sum_{\ell=0}^{L} B_\ell[r_1,r_2]P_\ell(\cos(\varphi_1-\varphi_2)). \tag{4.7}$$

Since the Legendre polynomials are orthonormal functions of $\varphi = \varphi_1-\varphi_2$, we can determine the coefficients $B_\ell[r_1,r_2]$ from (4.7). Thus, we can conclude that no information is lost from taking the projected second moment. ∎

Corollary 4.2. *Assume a function of the form*

$$f[r] = \sum_{\ell=0}^{L} \sum_{m=-\ell}^{\ell} A_\ell^m[r] Y_\ell^m.$$

Then, the second moment of the cryo-EM model (1.3) *is given by* (4.4)*. Therefore, the second moment determines the coefficient matrices* A_ℓ, $\ell = 0, \dots, L$, *up to the action of the ambiguity group* $\prod_{\ell=0}^{L} U(2\ell+1)$*. Moreover, if we consider functions* $f[r]$*, which are the Fourier transforms of real-valued functions on* $\mathbb{R}^3$ *(which is the scenario in cryo-EM), then the coefficients* $A_\ell^m[r]$ *are real for even* ℓ *and purely imaginary for odd* ℓ [25]*, and the ambiguity group is* $\prod_{\ell=0}^{L} O(2\ell+1)$*.*

4.3. Recovery of sparse structures from the second moment. Based on Theorem 3.1, we now prove that, in cryo-EM, a K-sparse signal can be recovered from the second moment when $K \lessapprox N/3$.

Theorem 4.3. *Assume a function of the form* (4.1)*, where the number of shells satisfies* $R \geq 2L+1$*. Let* $V = \oplus_{\ell=0}^{L} V_\ell^R$*, and let* $N = \dim V$*. Then, if*

$$\frac{K}{N} \leq \frac{2/3L^3 + L^2 + L/3}{2L^3 + 5L^2 + 4L + 1} \approx \frac{1}{3},$$

for a generic choice of orthonormal basis $\mathcal{V}$*, a generic* K*-sparse function* $f \in V$ *is uniquely determined by its second moment up to a global phase.*

Proof. The dimension of the representation V is $N = R(L+1)^2$. Thus, if $R \geq 2L+1$, then $N = \dim V \geq 2L^3 + 5L^2 + 4L + 1$. On the other hand, since $R \geq \dim V_\ell$ for all ℓ, we know by Proposition 3.5 that, for $f \in V$, the linear span $\mathbb{L}_f$ of the orbit of f under the ambiguity group $\oplus_{\ell=0}^{L} O(2\ell+1)$ has dimension at most

$$\sum_{\ell=0}^{L} (2\ell+1)^2 = 4/3L^3 + 4L^2 + 11L/3 + 1.$$

Therefore, by Theorem 3.1, if $K \leq 2/3L^3 + L^2 + L/3$, then, for a generic choice of orthonormal basis, a generic K-sparse vector $f \in V$ is uniquely determined by its second moment. ∎

Corollary 4.4. *Under the conditions of Theorem* 4.3*, a three-dimensional structure of the form* (4.1) *can be recovered from* n *realization from the cryo-EM model when* $n = \omega(\sigma^4)$*.*

Remark 4.5 (near-optimality). While the sparsity level of Theorem 4.3 is not necessarily optimal, it is optimal up to a constant. Thus, we say that our sparsity bound is near-optimal.

Remark 4.6. A recent paper [23] showed that a three-dimensional structure composed of a finite number of ideal point masses (or its convolution with a fixed kernel with a nonvanishing Fourier transform) can be recovered from the second moment. Theorem 4.3 is far more general because it includes sparse structures under almost any basis. Yet, [23] also suggests an algorithm that harnesses sparsity in the wavelet domain, for which our result does not necessarily hold (since Theorem 4.3 holds for generic bases, and we cannot verify that any particular basis satisfies the generic condition).

Remark 4.7 (spherical-Bessel expansion). Our analysis assumes a model of multiple shells as in (4.1). However, a similar analysis can be carried out to related models, such as spherical-Bessel expansion, where the coefficients $A_\ell^m[r]$ are expanded by

$$A_\ell^m[r] = \sum_{s=1}^{S_\ell} \tilde{A}_\ell^m[s] j_{\ell,s}[r],$$

where the $j_{\ell,s}[r]$ are the normalized spherical-Bessel functions. The "bandlimit" S_ℓ is determined by a sampling criterion, akin to the Nyquist sampling criterion [26]. This expansion has been useful in various cryo-EM tasks; see, for example, [60, 16, 24]. Our analysis can be applied to molecular structures represented using the spherical-Bessel expansion, where the only difference is the way we count the dimension of the representation.

5. Crystallographic phase retrieval.

The crystallographic phase retrieval problem is the problem of recovering a signal in $\mathbb{R}^N$ or $\mathbb{C}^N$ from its power spectrum. As seen from section 2.4.1, this is equivalent to recovering a signal from its second moment for the action of either the cyclic group $\mathbb{Z}_N$ or the dihedral group. However, because each irreducible representation appears exactly once, Theorem 3.1 provides an uninformative bound of $K \leq 0$.

In [18], the authors conjectured that, when $\mathbb{R}^N$ is given by the standard basis, a generic K-sparse vector in $\mathbb{R}^N$ can be recovered, up to unavoidable ambiguities, from its power spectrum if $K \leq N/2$ and the support is not an arithmetic progression. This conjecture was proved for a few specific cases, but a complete proof of this conjecture is beyond current techniques. In [46], it was shown that, for large enough N, K-sparse, symmetric signals are determined uniquely from their power spectrum for $K = O(N/\log^5 N)$.

On the other hand, for generic bases, the following provable optimal bound for phase retrieval was recently obtained [39] using the techniques of this paper. Unlike the conjectures of [18], this result makes no assumption on the support of the signal with respect to the given basis.

Theorem 5.1 ([39, Theorem 1.1]). *Let $\mathcal{V}$ be a generic basis for $\mathbb{R}^N$. Then, if $K \leq N/2$, a generic K-sparse vector can be recovered from its power spectrum up to a global phase.*

6. Discussion and future work.

In this paper, we have derived general sparsity conditions under which the sample complexity of the MRA model (1.1) is only $n = \omega(\sigma^4)$ rather than $n = \omega(\sigma^6)$ in the general case. We have further applied the result to cryo-EM, showing that, if a molecular structure can be represented with $\sim N/3$ coefficients in a generic basis, then the sample complexity is quadratic in the variance of the noise. Next, we delineate a few possible extensions of these results.

Linear transformations that are not compact groups. Our MRA model (1.1) assumes a compact group. However, in some important situations, the group is noncompact, for instance, the group of rigid motions SE(d) [21]. One challenge of working with noncompact groups is that their representations do not necessarily decompose into a sum of irreducibles, which makes the representation-theoretic analysis of the second moment more difficult. The problem is even more challenging when considering a combination of a group action with a general linear operator; this is, for example, the situation when considering subpixel measurements [22].

Sample complexity for specific bases. Our main theoretical result, Theorem 3.1, holds for almost all bases, but it is very difficult to say if it holds for a specific basis, such as wavelets, since the algebraic conditions on the bases are implicit. An important future work is to derive conditions for recovery from the second moment for specific bases, and ideally for all bases. (In [24], recovery from the second moment of structures composed of ideal point masses was proven.)

Unified theoretical framework with phase retrieval. In section 5, Theorem 5.1, we discussed sparsity conditions for recovering a signal from its power spectrum, which is the second moment of the simplest MRA model, where a signal in $\mathbb{R}^N$ is acted upon by $\mathbb{Z}_N$. This problem is called the phase retrieval problem. We wish to consolidate the proof techniques of Theorem 3.1 and those used to prove Theorem 5.1 in one general theoretical framework, which should yield optimal dimension bounds for recovering a signal from its second moment.

Multitarget detection. The multitarget detection model was devised to design a new computational paradigm for recovering small molecular structures using cryo-EM [15]. Without delving into the technical details, the second moment of this model is provided by the diagonals of the matrices B_ℓ, $\ell = 0, \dots, L$, which describe the second moment of the cryo-EM model (4.4) [16]. Deriving the conditions for signal recovery from these diagonals will have important implications for the sample complexity of the multitarget detection model and for understanding the fundamental limitations of cryo-EM technology.

Alternative priors. This work shows that the sample complexity of MRA and cryo-EM can be significantly improved if the signal can be sparsely represented. An interesting future research thread is studying alternative priors that can improve the sample complexity, such as statistical priors, data-driven priors (e.g., based on AlphaFold [53]), semialgebraic priors [37], or priors based on the statistical properties of proteins [90, 83].

Acknowledgments. We thank Nicolas Boumal for his notes on [54] and Guy Sharon and Oscar Mickelin for helping, respectively, with Figure 2 and Figure 3.

REFERENCES

[1] A. Abas, T. Bendory, and N. Sharon, *The generalized method of moments for multi-reference alignment*, IEEE Trans. Signal Process., 70 (2022), pp. 1377–1388.

[2] E. Abbe, T. Bendory, W. Leeb, J. M. Pereira, N. Sharon, and A. Singer, *Multireference alignment is easier with an aperiodic translation distribution*, IEEE Trans. Inform. Theory, 65 (2018), pp. 3565–3584.

[3] E. Abbe, J. M. Pereira, and A. Singer, *Estimation in the group action channel*, in 2018 IEEE International Symposium on Information Theory (ISIT), IEEE, 2018, pp. 561–565.

[4] C. Aguerrebere, M. Delbracio, A. Bartesaghi, and G. Sapiro, *Fundamental limits in multi-image alignment*, IEEE Trans. Signal Process., 64 (2016), pp. 5707–5722.

[5] Y. Aizenbud, B. Landa, and Y. Shkolnisky, *Rank-one multi-reference factor analysis*, Stat. Comput., 31 (2021), 8.

[6] K. Atkinson and W. Han, *Spherical Harmonics and Approximations on the Unit Sphere: An Introduction*, Lecture Notes in Math. 2044, Springer, Cham, 2012.

[7] A. S. Bandeira, B. Blum-Smith, J. Kileel, J. Niles-Weed, A. Perry, and A. S. Wein, *Estimation under group actions: Recovering orbits from invariants*, Appl. Comput. Harmon. Anal., 66 (2023), pp. 236–319.

[8] A. S. Bandeira, M. Charikar, A. Singer, and A. Zhu, *Multireference alignment using semidefinite programming*, in Proceedings of the 5th Conference on Innovations in Theoretical Computer Science, 2014, pp. 459–470.

[9] A. S. Bandeira, Y. Chen, R. R. Lederman, and A. Singer, *Non-unique games over compact groups and orientation estimation in cryo-EM*, Inverse Problems, 36 (2020), 064002.
[10] A. S. Bandeira, J. Niles-Weed, and P. Rigollet, *Optimal rates of estimation for multi-reference alignment*, Math. Stat. Learn., 2 (2020), pp. 25–75.
[11] A. Bartesaghi, A. Merk, S. Banerjee, D. Matthies, X. Wu, J. L. Milne, and S. Subramaniam, *2.2 Å resolution cryo-EM structure of β-galactosidase in complex with a cell-permeant inhibitor*, Science, 348 (2015), pp. 1147–1151.
[12] S. Basu and Y. Bresler, *Uniqueness of tomography with unknown view angles*, IEEE Trans. Image Process., 9 (2000), pp. 1094–1106.
[13] T. Bendory, A. Bartesaghi, and A. Singer, *Single-particle cryo-electron microscopy: Mathematical theory, computational challenges, and opportunities*, IEEE Signal Process. Mag., 37 (2020), pp. 58–76.
[14] T. Bendory, R. Beinert, and Y. C. Eldar, *Fourier phase retrieval: Uniqueness and algorithms*, in Compressed Sensing and Its Applications, Springer, Cham, 2017, pp. 55–91.
[15] T. Bendory, N. Boumal, W. Leeb, E. Levin, and A. Singer, *Multi-target detection with application to cryo-electron microscopy*, Inverse Problems, 35 (2019), 104003.
[16] T. Bendory, N. Boumal, W. Leeb, E. Levin, and A. Singer, *Toward single particle reconstruction without particle picking: Breaking the detection limit*, SIAM J. Imaging Sci., 16 (2023), pp. 886–910.
[17] T. Bendory, N. Boumal, C. Ma, Z. Zhao, and A. Singer, *Bispectrum inversion with application to multireference alignment*, IEEE Trans. Signal Process., 66 (2017), pp. 1037–1050.
[18] T. Bendory and D. Edidin, *Toward a mathematical theory of the crystallographic phase retrieval problem*, SIAM J. Math. Data Sci., 2 (2020), pp. 809–839.
[19] T. Bendory and D. Edidin, *Algebraic theory of phase retrieval*, Notices AMS, 69 (2022), pp. 1487–1495.
[20] T. Bendory, D. Edidin, W. Leeb, and N. Sharon, *Dihedral multi-reference alignment*, IEEE Trans. Inform. Theory, 68 (2022), pp. 3489–3499.
[21] T. Bendory, I. Hadi, and N. Sharon, *Compactification of the rigid motions group in image processing*, SIAM J. Imaging Sci., 15 (2022), pp. 1041–1078.
[22] T. Bendory, A. Jaffe, W. Leeb, N. Sharon, and A. Singer, *Super-resolution multi-reference alignment*, Inf. Inference, 11 (2022), pp. 533–555.
[23] T. Bendory, Y. Khoo, J. Kileel, O. Mickelin, and A. Singer, *Autocorrelation analysis for cryo-EM with sparsity constraints: Improved sample complexity and projection-based algorithms*, Proc. Natl. Acad. Sci. USA, 120 (2023), e2216507120.
[24] T. Bendory, O. Michelin, and A. Singer, *Sparse multi-reference alignment: Sample complexity and computational hardness*, in ICASSP 2022-2022 IEEE International Conference on Acoustics, Speech and Signal Processing (ICASSP), IEEE, 2022, pp. 8977–8981.
[25] T. Bhamre, T. Zhang, and A. Singer, *Orthogonal matrix retrieval in cryo-electron microscopy*, in 2015 IEEE 12th International Symposium on Biomedical Imaging (ISBI), IEEE, 2015, pp. 1048–1052.
[26] T. Bhamre, T. Zhang, and A. Singer, *Anisotropic Twicing for Single Particle Reconstruction Using Autocorrelation Analysis*, preprint, arXiv:1704.07969, 2017.
[27] N. Boumal, *Nonconvex phase synchronization*, SIAM J. Optim., 26 (2016), pp. 2355–2377.
[28] N. Boumal, T. Bendory, R. R. Lederman, and A. Singer, *Heterogeneous multireference alignment: A single pass approach*, in 2018 52nd Annual Conference on Information Sciences and Systems (CISS), IEEE, 2018, pp. 1–6.
[29] V.-E. Brunel, *Learning rates for Gaussian mixtures under group action*, in Conference on Learning Theory, PMLR 99, 2019, pp. 471–491.
[30] E. J. Candès, J. Romberg, and T. Tao, *Robust uncertainty principles: Exact signal reconstruction from highly incomplete frequency information*, IEEE Trans. Inform. Theory, 52 (2006), pp. 489–509.
[31] H. Chen, M. Zehni, and Z. Zhao, *A spectral method for stable bispectrum inversion with application to multireference alignment*, IEEE Signal Process. Lett., 25 (2018), pp. 911–915.
[32] Y. Chen and E. J. Candès, *The projected power method: An efficient algorithm for joint alignment from pairwise differences*, Comm. Pure Appl. Math., 71 (2018), pp. 1648–1714.
[33] R. R. Coifman, Y. Shkolnisky, F. J. Sigworth, and A. Singer, *Graph Laplacian tomography from unknown random projections*, IEEE Trans. Image Process., 17 (2008), pp. 1891–1899.
[34] J. J. Donatelli, P. H. Zwart, and J. A. Sethian, *Iterative phasing for fluctuation X-ray scattering*, Proc. Natl. Acad. Sci. USA, 112 (2015), pp. 10286–10291.

[35] D. L. Donoho, *Compressed sensing*, IEEE Trans. Inform. Theory, 52 (2006), pp. 1289–1306.
[36] Z. Dou, Z. Fan, and H. Zhou, *Rates of Estimation for High-Dimensional Multi-reference Alignment*, preprint, arXiv:2205.01847, 2022.
[37] N. Dym and S. J. Gortler, *Low Dimensional Invariant Embeddings for Universal Geometric Learning*, preprint, arXiv:2205.02956, 2022.
[38] D. Edidin and M. Satriano, *Orbit Recovery for Band-Limited Functions*, preprint, arXiv:2306.00155, 2023.
[39] D. Edidin and A. Suresh, *The Generic Crystallographic Phase Retrieval Problem*, preprint, arXiv:2307.06835, 2023.
[40] M. Elad, *Sparse and Redundant Representations: From Theory to Applications in Signal and Image Processing*, Vol. 2, Springer, New York, 2010.
[41] Y. C. Eldar and G. Kutyniok, *Compressed Sensing: Theory and Applications*, Cambridge University Press, Cambridge, UK, 2012.
[42] C. Esteve-Yagüe, W. Diepeveen, O. Öktem, and C.-B. Schönlieb, *Spectral decomposition of atomic structures in heterogeneous cryo-EM*, Inverse Problems, 39 (2023), 034003.
[43] Z. Fan, R. R. Lederman, Y. Sun, T. Wang, and S. Xu, *Maximum Likelihood for High-Noise Group Orbit Estimation and Single-Particle Cryo-EM*, preprint, arXiv:2107.01305, 2021.
[44] Z. Fan, Y. Sun, T. Wang, and Y. Wu, *Likelihood landscape and maximum likelihood estimation for the discrete orbit recovery model*, Comm. Pure. Appl. Math., 76 (2023), pp. 1208–1302.
[45] J. Frank, *Three-Dimensional Electron Microscopy of Macromolecular Assemblies: Visualization of Biological Molecules in Their Native State*, Oxford University Press, Oxford, UK, 2006.
[46] S. Ghosh and P. Rigollet, *Sparse multi-reference alignment: Phase retrieval, uniform uncertainty principles and the beltway problem*, Found. Comput. Math., 23 (2023), pp. 1851–1898.
[47] I. Goodfellow, Y. Bengio, and A. Courville, *Deep Learning*, MIT Press, Cambridge, MA, 2016.
[48] P. Grohs, S. Koppensteiner, and M. Rathmair, *Phase retrieval: Uniqueness and stability*, SIAM Rev., 62 (2020), pp. 301–350.
[49] M. Hirn and A. Little, *Wavelet invariants for statistically robust multi-reference alignment*, Inf. Inference, 10 (2021), pp. 1287–1351.
[50] S. Huang, M. Zehni, I. Dokmanić, and Z. Zhao, *Orthogonal matrix retrieval with spatial consensus for 3D unknown view tomography*, SIAM J. Imaging Sci., 16 (2023), pp. 1398–1439.
[51] N. Janco and T. Bendory, *An accelerated expectation-maximization algorithm for multi-reference alignment*, IEEE Trans. Signal Process., 70 (2022), pp. 3237–3248.
[52] S. Jonić and C.Ó.S. Sorzano, *Coarse-graining of volumes for modeling of structure and dynamics in electron microscopy: Algorithm to automatically control accuracy of approximation*, IEEE J. Sel. Top. Signal Process., 10 (2015), pp. 161–173.
[53] J. Jumper, R. Evans, A. Pritzel, T. Green, M. Figurnov, O. Ronneberger, K. Tunyasuvunakool, R. Bates, A. Žídek, A. Potapenko, et al., *Highly accurate protein structure prediction with AlphaFold*, Nature, 596 (2021), pp. 583–589.
[54] Z. Kam, *The reconstruction of structure from electron micrographs of randomly oriented particles*, J. Theoret. Biol., 82 (1980), pp. 15–39.
[55] A. Katsevich and A. S. Bandeira, *Likelihood maximization and moment matching in low SNR Gaussian mixture models*, Comm. Pure Appl. Math., 76 (2023), pp. 788–842.
[56] T. Kawabata, *Gaussian-input Gaussian mixture model for representing density maps and atomic models*, J. Struct. Biol., 203 (2018), pp. 1–16.
[57] S. Kreymer, A. Singer, and T. Bendory, *An approximate expectation-maximization for two-dimensional multi-target detection*, IEEE Signal Process. Lett., 29 (2022), pp. 1087–1091.
[58] T.-Y. Lan, N. Boumal, and A. Singer, *Random conical tilt reconstruction without particle picking in cryo-electron microscopy*, Acta Crystallogr. Sect. A, 78 (2022), pp. 294–301.
[59] C.-H. Lee and R. MacKinnon, *Structures of the human HCN1 hyperpolarization-activated channel*, Cell, 168 (2017), pp. 111–120.
[60] E. Levin, T. Bendory, N. Boumal, J. Kileel, and A. Singer, *3D ab initio modeling in cryo-EM by autocorrelation analysis*, in 2018 IEEE 15th International Symposium on Biomedical Imaging (ISBI 2018), IEEE, 2018, pp. 1569–1573.

[61] S. Ling, *Near-optimal performance bounds for orthogonal and permutation group synchronization via spectral methods*, Appl. Comput. Harmon. Anal., 60 (2022), pp. 20–52.
[62] A. Liu and A. Moitra, *Algorithms from Invariants: Smoothed Analysis of Orbit Recovery over $SO(3)$*, preprint, arXiv:2106.02680, 2021.
[63] C. Ma, T. Bendory, N. Boumal, F. Sigworth, and A. Singer, *Heterogeneous multireference alignment for images with application to 2D classification in single particle reconstruction*, IEEE Trans. Image Process., 29 (2019), pp. 1699–1710.
[64] F. R. Maia and J. Hajdu, *The trickle before the torrent—Diffraction data from X-ray lasers*, Sci. Data, 3 (2016), 160059.
[65] S. Mallat, *A Wavelet Tour of Signal Processing*, Elsevier, Amsterdam, 1999.
[66] F. Natterer, *The Mathematics of Computerized Tomography*, SIAM, Philadelphia, 2001.
[67] T. H. D. Nguyen, W. P. Galej, X.-c. Bai, C. Oubridge, A. J. Newman, S. H. Scheres, and K. Nagai, *Cryo-EM structure of the yeast U4/U6.U5 tri-snRNP at 3.7 Å resolution*, Nature, 530 (2016), pp. 298–302.
[68] E. Nogales, *The development of cryo-EM into a mainstream structural biology technique*, Nat. Methods, 13 (2016), pp. 24–27.
[69] K. Pearson, *Contributions to the mathematical theory of evolution*, Philos. Trans. Roy. Soc. Lond. A, 185 (1894), pp. 71–110.
[70] A. Perry, J. Weed, A. S. Bandeira, P. Rigollet, and A. Singer, *The sample complexity of multireference alignment*, SIAM J. Math. Data Sci., 1 (2019), pp. 497–517.
[71] T. Pumir, A. Singer, and N. Boumal, *The generalized orthogonal Procrustes problem in the high noise regime*, Inf. Inference, 10 (2021), pp. 921–954.
[72] A. Punjani, J. L. Rubinstein, D. J. Fleet, and M. A. Brubaker, *cryoSPARC: Algorithms for rapid unsupervised cryo-EM structure determination*, Nat. Methods, 14 (2017), pp. 290–296.
[73] E. Romanov, T. Bendory, and O. Ordentlich, *Multi-reference alignment in high dimensions: Sample complexity and phase transition*, SIAM J. Math. Data Sci., 3 (2021), pp. 494–523.
[74] D. M. Rosen, L. Carlone, A. S. Bandeira, and J. J. Leonard, *SE-Sync: A certifiably correct algorithm for synchronization over the special Euclidean group*, Int. J. Rob. Res., 38 (2019), pp. 95–125.
[75] D. Saldin, V. Shneerson, M. R. Howells, S. Marchesini, H. N. Chapman, M. Bogan, D. Shapiro, R. Kirian, U. Weierstall, K. Schmidt, et al., *Structure of a single particle from scattering by many particles randomly oriented about an axis: Toward structure solution without crystallization?*, New J. Phys., 12 (2010), 035014.
[76] S. H. Scheres, *RELION: Implementation of a Bayesian approach to cryo-EM structure determination*, J. Struct. Biol., 180 (2012), pp. 519–530.
[77] N. Sharon, J. Kileel, Y. Khoo, B. Landa, and A. Singer, *Method of moments for 3D single particle ab initio modeling with non-uniform distribution of viewing angles*, Inverse Problems, 36 (2020), 044003.
[78] Y. Shechtman, Y. C. Eldar, O. Cohen, H. N. Chapman, J. Miao, and M. Segev, *Phase retrieval with application to optical imaging: A contemporary overview*, IEEE Signal Process. Mag., 32 (2015), pp. 87–109.
[79] Y. Shkolnisky and A. Singer, *Viewing direction estimation in cryo-EM using synchronization*, SIAM J. Imaging Sci., 5 (2012), pp. 1088–1110.
[80] F. J. Sigworth, *A maximum-likelihood approach to single-particle image refinement*, J. Struct. Biol., 122 (1998), pp. 328–339.
[81] A. Singer, *Angular synchronization by eigenvectors and semidefinite programming*, Appl. Comput. Harmon. Anal., 30 (2011), pp. 20–36.
[82] A. Singer, *Mathematics for cryo-electron microscopy*, in Proceedings of the International Congress of Mathematicians: Rio de Janeiro 2018, World Scientific, 2018, pp. 3995–4014.
[83] A. Singer, *Wilson statistics: Derivation, generalization and applications to electron cryomicroscopy*, Acta Crystallogr. A Found. Adv., 77 (2021), pp. 472–479.
[84] A. Singer and Y. Shkolnisky, *Three-dimensional structure determination from common lines in cryo-EM by eigenvectors and semidefinite programming*, SIAM J. Imaging Sci., 4 (2011), pp. 543–572.

[85] A. Singer and F. J. Sigworth, *Computational methods for single-particle electron cryomicroscopy*, Annu. Rev. Biomed. Data Sci., 3 (2020), 163.
[86] A. Singer and H.-T. Wu, *Two-dimensional tomography from noisy projections taken at unknown random directions*, SIAM J. Imaging Sci., 6 (2013), pp. 136–175.
[87] J. C. Spence, U. Weierstall, and H. Chapman, *X-ray lasers for structural and dynamic biology*, Rep. Prog. Phys., 75 (2012), 102601.
[88] R. Tibshirani, *Regression shrinkage and selection via the lasso*, J. R. Stat. Soc. Ser. B. Stat. Methodol., 58 (1996), pp. 267–288.
[89] C. Vonesch, L. Wang, Y. Shkolnisky, and A. Singer, *Fast wavelet-based single-particle reconstruction in cryo-EM*, in 2011 IEEE International Symposium on Biomedical Imaging: From Nano to Macro, IEEE, 2011, pp. 1950–1953.
[90] A. Wilson, *The probability distribution of X-ray intensities*, Acta Crystallogr., 2 (1949), pp. 318–321.
[91] W. Wong, X.-c. Bai, A. Brown, I. S. Fernandez, E. Hanssen, M. Condron, Y. H. Tan, J. Baum, and S. H. Scheres, *Cryo-EM structure of the Plasmodium falciparum* 80*S ribosome bound to the anti-protozoan drug emetine*, Elife, 3 (2014), e03080.
[92] M. Zehni, S. Huang, I. Dokmanić, and Z. Zhao, 3*D unknown view tomography via rotation invariants*, in ICASSP 2020, 2020 IEEE International Conference on Acoustics, Speech and Signal Processing (ICASSP), IEEE, 2020, pp. 1449–1453.
[93] M. Zehni and Z. Zhao, *An adversarial learning based approach for* 2*D unknown view tomography*, IEEE Trans. Comput. Imaging, 8 (2022), pp. 705–720.